(12) INTERNATIONAL APPLICATION PUBLISHED UNDER THE PATENT COOPERATION TREATY (PCT)

(19) World Intellectual Property Organization
International Bureau

(43) International Publication Date
23 April 2026 (23.04.2026)

WIPO | PCT

(10) International Publication Number
WO 2026/085288 A1

(51) International Patent Classification:
G01N 33/68 (2006.01) *A61K 39/39* (2006.01)
G01N 1/40 (2006.01)

(21) International Application Number:
PCT/US2025/051190

(22) International Filing Date:
16 October 2025 (16.10.2025)

(25) Filing Language: English

(26) Publication Language: English

(30) Priority Data:
63/708,017 16 October 2024 (16.10.2024) US

(71) Applicant: **WISCONSIN ALUMNI RESEARCH FOUNDATION** [US/US]; 614 Walnut Street, 13th Floor, Madison, Wisconsin 53726 (US).

(72) Inventors: **HU, Quanyin**; 1101 Dolan Ave, Waunakee, Wisconsin 53597 (US). **LI, Zhaoting**; 2001 Longxiang Boulevard, Longgang District, Shenzhen, Guangdong 518172 (CN).

(74) Agent: **LECUYER, Karen A.** et al.; 25 W. Main Street, Suite 800, Madison, Wisconsin 53703 (US).

(81) Designated States *(unless otherwise indicated, for every kind of national protection available)*: AE, AG, AL, AM, AO, AT, AU, AZ, BA, BB, BG, BH, BN, BR, BW, BY, BZ, CA, CH, CL, CN, CO, CR, CU, CV, CZ, DE, DJ, DK, DM, DO, DZ, EC, EE, EG, ES, FI, GB, GD, GE, GH, GM, GT, HN, HR, HU, ID, IL, IN, IQ, IR, IS, IT, JM, JO, JP, KE, KG, KH, KN, KP, KR, KW, KZ, LA, LC, LK, LR, LS, LU, LY, MA, MD, MG, MK, MN, MU, MW, MX, MY, MZ, NA, NG, NI, NO, NZ, OM, PA, PE, PG, PH, PL, PT, QA, RO, RS, RU, RW, SA, SC, SD, SE, SG, SK, SL, ST, SV, SY, TH, TJ, TM, TN, TR, TT, TZ, UA, UG, US, UY, UZ, VC, VN, WS, ZA, ZM, ZW.

(84) Designated States *(unless otherwise indicated, for every kind of regional protection available)*: ARIPO (BW, CV, GH, GM, KE, LR, LS, MU, MW, MZ, NA, RW, SC, SD, SL, ST, SZ, TZ, UG, ZM, ZW), Eurasian (AM, AZ, BY, KG, KZ, RU, TJ, TM), European (AL, AT, BE, BG, CH, CY, CZ, DE, DK, EE, ES, FI, FR, GB, GR, HR, HU, IE, IS, IT, LT, LU, LV, MC, ME, MK, MT, NL, NO, PL, PT, RO, RS, SE, SI, SK, SM, TR), OAPI (BF, BJ, CF, CG, CI, CM, GA, GN, GQ, GW, KM, ML, MR, NE, SN, TD, TG).

Published:
— *with international search report (Art. 21(3))*
— *before the expiration of the time limit for amending the claims and to be republished in the event of receipt of amendments (Rule 48.2(h))*
— *with sequence listing part of description (Rule 5.2(a))*

(54) Title: TUMOR-DERIVED EXTRACELLUAR VESICLES, METHODS OF MAKING, AND METHODS OF USE THEREOF

(57) Abstract: Described here is an extracellular vesicle termed pyosomes and methods of preparing them. A method of preparing isolated pyosomes includes providing an *ex-vivo* tumor cell, treating the tumor cell with a pyroptosis-inducing agent under conditions for the tumor cell to undergo pyroptosis and produce pyosomes, and isolating the pyosomes from the treated tumor cells. The product of the foregoing process is also included. Also described is an immunostimulant composition wherein the pyosomes are loaded with an immunostimulant compound. The immunostimulant composition can be in the form of a pharmaceutical composition such as an implantable pharmaceutical composition. Further described are methods of treating a patient in need of treatment for solid tumors or post-surgical tumor recurrence by administering to the patient the immunostimulant composition.

WO 2026/085288 A1

TUMOR-DERIVED EXTRACELLULAR VESICLES, METHODS OF MAKING, AND METHODS OF USE THEREOF

CROSS-REFERENCE TO RELATED APPLICATIONS

This application claims priority to U.S. Provisional Application 63/708,017 filed on October 16, 2024, which is incorporated herein by reference in its entirety.

SEQUENCE LISTING

The Instant Application contains a Sequence Listing which has been submitted electronically in XML format and is hereby incorporated by reference in its entirety. Said XML copy, created on October 9, 2025, is named "SEQ_LIST--107668337-P250007WO01.xml" and is 2,837 bytes in size. The Sequence Listing does not go beyond the disclosure in the application as filed.

FIELD OF THE DISCLOSURE

[0001] The present disclosure is related to tumor-derived extracellular vesicles, methods of making tumor-derived extracellular vesicles, and their compositions and use to treat cancer, particularly solid tumors.

BACKGROUND

[0002] Tumor vaccines offer opportunities to address post-surgical tumor recurrence and metastasis by evoking local and systemic anti-tumor immune responses to eradicate residual and metastasized tumor cells. They have achieved promising outcomes in clinical trials for treating solid tumors such as malignant melanoma, lung cancer, and ovarian cancer. Nevertheless, current tumor vaccines have several limitations restricting their further application. The diversity of tumor neoepitopes among individuals results in variable responses to a universal tumor vaccine. Due to tumor heterogeneity, vaccines targeting a single antigen cannot induce multivalent immune responses to eradicate all tumor cells. Some tumor vaccines may induce severe side effects associated with excessive or non-specific immune responses, risking patients' lives. Given the fact that tumor antigens are critical to determining cancer vaccination outcomes, significant efforts have been made to develop or identify tumor antigens that are shared among patients and hold the potential to elicit strong tumor-specific immune responses. As an emerging strategy, developing vaccines using materials derived from the tumor patients themselves presents another

approach for customizing personalized vaccines. Unlike traditional one-size-fits-all vaccination methods, these materials, such as whole tumor cells or their extracellular vesicles (EVs), display a set of tumor-associated antigens/neoantigens and empower the production of customized tumor vaccines to combat the heterogeneous antigen expression on each patient's tumor.

[0003] Among all tumor cell-based vaccines, using tumor-derived EVs as building blocks for tumor vaccines represents a promising approach for personalized vaccination. EVs, such as exosomes, microvesicles, and apoptotic bodies, are membrane-bound nanoscale or microscale particles shedding from cells. These vesicles play critical roles in cell-to-cell communication by ferrying a multitude of biological molecules such as proteins, lipids, and nucleic acids. Notably, with the ability to transport tumor antigens, they have emerged as promising candidates for developing tumor vaccines. EVs derived from tumor cells pack a broad spectrum of antigens/neoantigens, which can overcome the hurdles associated with identifying specific antigens. Furthermore, due to the multivalent nature of EVs, a single EV possesses multiple types of antigens, providing broad prospects for addressing the common heterogeneity of overall immune responses in tumors. As an endogenous structure, EVs exhibited better biocompatibility than synthetic delivery vectors, which may reduce the risk of adverse immune reactions. Tumor EV-based vaccines have shown potential in inducing anti-tumor immune responses in clinical trials; however, their therapeutic efficacy is generally suboptimal. Despite the enormous therapeutic potential, the tumor-derived EVs that have been explored by far still have certain limitations. Since these EVs originate from the tumor itself, they may have immune evasion mechanisms, such as overexpression of PD-L1 ligands, to support tumor progression. In addition, tumor-derived EVs can inadvertently transfer carcinogenic molecules to healthy cells, posing a risk of malignant transformation and tumorigenesis.

[0004] What is needed are new methods to generate tumor-derived EVs that overcome the disadvantages of prior art EVs.

BRIEF SUMMARY

[0005] In an aspect, a method of preparing isolated pyosomes comprises providing an *ex-vivo* tumor cell, treating the tumor cell with a pyroptosis-inducing agent under conditions for the tumor cell to undergo pyroptosis and produce pyosomes, and isolating the pyosomes from the treated tumor cells. The product of the foregoing process is also included.

[0006] In another aspect, also included is an immunostimulant composition comprising the pyosomes loaded with an immunostimulant compound. The immunostimulant composition can be in the form of a pharmaceutical composition such as an implantable pharmaceutical composition.

[0007] In an aspect, a method of treating a patient in need of treatment for a solid tumor comprises administering to the patient the pharmaceutical composition described above. In an aspect, the pyosomes are prepared from tumor cells isolated from the patient.

BRIEF DESCRIPTION OF THE DRAWINGS

[0008] FIGs. 1a-h show the observation and identification of pyosomes. The arrows indicate vesicle formation. FIG. 1a. Representative scanning electron microscope (SEM) images showing the pyosome formation in 4T1 cells. Scale bar = 10 μm. FIG. 1b. Confocal microscopy images of the pyosome formation in 4T1 cells. Cells were stained with wheat germ agglutinin (WGA)-Rhodamine B and Hoechst 33342. Scale bar = 10 μm. FIG. 1c. Representative SEM images of normal 4T1 cells. Scale bar = 10 μm. FIG. 1d. Confocal microscopy images of normal 4T1 cells. Scale bar = 10 μm. FIG. 1e. Representative SEM images showing the pyosome formation in B16F10 cells. Scale bar = 2 μm. FIG. 1f. Confocal microscopy images of the pyosome formation in B16F10 cells. Scale bar = 10 μm. FIG. 1g. Representative SEM images of normal B16F10 cells. Scale bar = 3 μm. FIG. 1h. Confocal microscopy images of normal B16F10 cells. Scale bar = 10 μm.

[0009] FIGs. 2a-n show extraction and characterization of the pyosomes. FIG. 2a. Schematic illustration of the formation and extraction of the pyosomes. FIGs. 2b, 2c. Lactate dehydrogenase (LDH) release from the 4T1 (2b) and B16F10 (2c) cells after pyroptosis. Data are shown as mean ± s.d. (n = 5) and analyzed with unpaired *t*-test. $****P < 0.0001$. FIGs. 2d, 2e. SYTOX™ Green (2d) and PI (2e) staining analysis of the 4T1 cells after different treatments. FIGs. 2f, 2g. SYTOX™ Green (2f) and PI (2g) staining analysis of the B16F10 cells after different treatments. FIGs. 2h, 2i. Western Blot analysis of the 4T1 cells (2h) and B16F10 cells (i) after pyroptosis. FIGs. 2j, 2k. Particle size distribution (2j) and analysis (2k) of the 4T1 and B16F10 pyosomes. FIG. 2l, SEM imaging of the extracted 4T1 pyosomes. Scale bar = 500 nm. FIG. 2m, TEM imaging of the extracted 4T1 pyosomes. Scale bar = 500 nm. FIG. 2n. Zeta potential analysis of the pyosomes from 4T1 and B16F10 cells.

[0010] FIGs. 3a-f show protein and microRNA analysis of pyosomes. FIG. 3a. Protein compositions in 4T1 tumor pyosomes and exosomes. FIG. 3b. Volcano plot analysis

of the proteins from 4T1 pyosomes (Pyo) in comparison to 4T1 tumor exosomes (Exo). FIG. 3c. Heatmap of representative protein expressions in 4T1 tumor pyosomes and exosomes. FIG. 3d. Volcano plot analysis of the microRNAs from 4T1 pyosomes (Pyo) in comparison to 4T1 tumor exosomes (Exo). FIG. 3e. Heatmap analysis of the relative expression level of the detailed microRNAs in 4T1 pyosomes and exosomes. FIG. 3f. Enrichment plot of the microRNAs in different signaling pathways.

[0011] FIGs. 4a-h show anti-tumor efficacy of the pyosome vaccine in mouse 4T1 metastatic triple negative breast cancer (TNBC) and B16F10 melanoma models. FIG. 4a. Region-of-interest analysis of bioluminescence intensity in IVIS images of the 4T1-Luc tumor recurrence after the treatment of the pyosome vaccine (n = 6 mice). Data are shown as mean ± s.d. and analyzed with two-way ANOVA followed by Dunnett's multiple comparison test. FIG. 4b. Survival curve of the 4T1 tumor recurrence mouse model after various treatments (n = 6 mice). Data are analyzed with Log-rank (Mantel-Cox) test. FIG. 4c. Number of lung metastatic nodules after various treatments (n = 4 independent samples). Data are shown as mean ± s.d. and analyzed with one-way ANOVA followed by Dunnett's multiple comparison test. FIG. 4d. Lung images after various treatments (n = 4 independent samples). Scale bar = 2 mm. FIG. 4e. Hematoxylin & eosin (H&E) analysis of the lung metastasis after various treatments (n = 4 independent samples). Scale bar = 2 mm. FIG. FIG. 4f. Schematic illustration of the experimental schedule of the B16F10 melanoma double tumor model. FIG. 4g. Tumor growth curve of the distant tumor after the implantation of various treatments at the primary surgical bed (n = 6 mice). Data are shown as mean ± s.d. and analyzed with two-way ANOVA followed by Dunnett's multiple comparison test. FIG. 4h. Survival curve of the distant tumor mouse model after the implantation of various treatments at the primary surgical bed (n = 6 mice). Data are analyzed with the Log-rank (Mantel-Cox) test. $^{**}P < 0.01$; $^{***}P < 0.001$.

[0012] FIGs. 5a-h show *in vitro* and *in vivo* immune activation by the pyosome vaccine. FIGs. 5a, 5b. Representative flow cytometry plots of the CD80 (5a) and CD86 (5b) expression on the BMDCs after different treatments in vitro. FIGs. 5c, 5d. Data analysis of the CD80 (5c) and CD86 (5d) expression on the BMDCs after different treatments in vitro. FIG. 5e, 5f. ELISA analysis of the quantitative concentrations of TNFα (5e) and IL-12p70 (5f) in the supernatant of DCs after different treatments *in vitro* (n = 3 independent samples). FIG. 5g. CD80 and CD86 expression on DCs in the lymph nodes detected by flow cytometry after different treatments in vivo. FIG. 5h. The percentage of $CD3^+CD8^+$ T cell infiltration in the tumor tissues detected by flow cytometry after different treatments in vivo. Data are

shown as mean ± s.d. (n = 3) and analyzed with one-way ANOVA followed by Dunnett's multiple comparison test. *$P < 0.05$; **$P < 0.01$; ***$P < 0.001$.

[0013] FIGs 6a-h show evaluation of the antigen-specific immune activation. FIG. 6a. Representative plots showing ovalbumin (OVA)-specific DC activation detected by the flow cytometry of the H-2Kb (SIINFEKL; SEQ ID NO: 1) expression on $CD11c^+$ DCs in the lymph nodes (n = 5 mice). FIG. 6b. Representative plots showing OVA-specific T cell activation detected by the flow cytometry of the SIINFEKL; SEQ ID NO: 1 Tetramer staining (n = 5 mice). FIG. 6c. Data analysis of the H-2Kb (SIINFEKL) expression on $CD11c^+$ DCs. FIG. 6d. Data analysis of SIINFEKL $Tetramer^+$ $CD8^+$ T cells. FIGs. 6e, 6f. Data analysis of the MC38 tumor neoantigen-specific T cell activation detected by the flow cytometry of the Adpgk $Tetramer^+$ $CD8^+$ T cells in the blood (6e) and tumor tissue (6f) (n = 5 mice). FIGs. 6g, 6h. Representative flow cytometry plots showing MC38 tumor neoantigen-specific T cell activation by analysis of the Adpgk $Tetramer^+$ $CD8^+$T cells in the blood (6g) and tumor tissue (6h). Data are shown as mean ± s.d. (n = 5) and analyzed with one-way ANOVA followed by Dunnett's multiple comparison test. *$P < 0.05$; **$P < 0.01$; ***$P < 0.001$.

[0014] FIGs 7a-h show verification of pyosome formation in human triple negative breast cancer (TNBC) cells and therapeutic evaluation of pyosome vaccines in humanized PDX TNBC-bearing mouse model. FIG. 7a. Representative confocal microscopy images of the pyosome formation in MDA-MB-231 cells. Scale bar = 10 μm. FIGs. 7b, 7c. SYTOX™ Green (7b) and PI (7c) staining assay of the pyroptotic MDA-MB-231 cells. FIG. 7d. Particle size distribution of the extracted MDA-MB-231 pyosomes. FIG. 7e. Schematic illustration of the establishment of the PDX TNBC model on humanized mice and the personalized vaccination strategy. FIG. 7f. Representative image of the collected tumor tissues after different treatments (scale bar = 1 cm). FIGs. 7g, 7h. Tumor volume (7g) and tumor weight (7h) of the collected tumor tissues after different treatments. Data are shown as mean ± s.d. (n = 3) and analyzed with one-way ANOVA followed by Dunnett's multiple comparison test. *$P < 0.05$; ***$P < 0.001$.

[0015] FIG. 8 is a schematic illustration of the preparation and application of the personalized pyosome vaccines.

[0016] The above-described and other features will be appreciated and understood by those skilled in the art from the following detailed description, drawings, and appended claims.

DETAILED DESCRIPTION

[0017] In an aspect, described herein a type of EV (designated pyosomes) which can be engineered for personalized cancer vaccines. Pyosomes are vesicles generated from tumor cells undergoing pyroptosis, which is a form of inflammatory programmed cell death characterized by cellular swelling, plasma membrane rupture, and inflammatory responses. This unique process culminates in the formation of vesicle-like pyosomes, which are rich in immunogenic content. The advantage of pyosomes lies in their natural composition of cellular remnants replete with tumor-specific antigens and danger-associated molecular patterns (DAMPs). Pyosomes can replicate the antigen composition of their homologous tumors, in which some tumor antigens can hardly be identified, thus activating immune responses against complex and heterogeneous tumors. Equipped with multiple tumor antigens and immunogenic cellular remnants, the pyosome has the potential to serve as a tumor vaccine platform to orchestrate robust anti-tumor immune responses. As described herein, pyosomes were isolated from pyroptotic tumor cells, and their physicochemical properties, intracellular biomolecular contents, and immune activation capability were comprehensively evaluated in vitro. To evaluate pyosomes' vaccination capability against post-surgical tumor recurrence, pyosomes were engineered with the encapsulation of the immunostimulant resiquimod and further embedded into a biocompatible hyaluronic acid (HA) hydrogel that can be implanted into the post-surgical tumor cavity. The released pyosomes at the tumor site could recruit and activate dendritic cells (DCs), which present tumor antigens to T cells and provoke an anti-tumor response to eliminate residual tumor cells and prevent tumor recurrence. The anti-tumor recurrence efficacy was demonstrated on multiple cancer models, including the subcutaneous B16F10 melanoma, orthotopic 4T1 TNBC, and PDX TNBC-bearing humanized mouse models. Furthermore, the antigen-specific immune responses were validated on an artificial OVA antigen on the OVA-B16F10 tumor model and a neoantigen Adpgk (a single-epitope mutation within Adpgk protein) on the MC38 tumor model. Pyosomes can be customized as personalized tumor vaccines to treat individual patients.

[0018] As used herein, pyroptosis is a form of inflammatory programmed cell death stimulated by inflammasome activation and characterized by cellular swelling, plasma membrane rupture, and inflammatory responses. Cells undergoing pyroptosis are characterized by typical morphological changes, such as swelling and large protrusions. Pyroptotic cells also undergo membrane rupture which can be monitored by measuring release of lactate dehydrogenase (LDH). A pyroptosis-inducing agent is an agent that, when

contacted with a cell, causes the cell to undergo pyroptosis. A pyosome is an extracellular vesicle produced when a cell is treated to undergo pyroptosis.

[0019] In an aspect, a method of preparing isolated pyosomes comprises providing an *ex-vivo* tumor cell, treating the tumor cell with a pyroptosis-inducing agent under conditions for the tumor cell to undergo pyroptosis and produce pyosomes, and isolating the pyosomes from the treated tumor cells.

[0020] Tumor cells include cultured tumor cells as well as tumor cells isolated from a patient. Preferred tumor cells to prepare pyosomes for therapeutic applications are tumor cells isolated from a patient, particularly solid tumor cells. Solid tumor cells can be isolated, for example, from a solid biopsy from a patient with cancer. Exemplary tumor cells include solid tumor cells such as cells from a patient with triple negative breast cancer, malignant melanoma, lung cancer, ovarian cancer, colon cancer, prostate cancer, bladder cancer, sarcomas, lymphomas which produce solid tumors, liver cancer, and the like.

[0021] The tumor cell is treated with a pyroptosis-inducing agent under conditions for the tumor cell to undergo pyroptosis and produce pyosomes. Exemplary pyroptosis-inducing agents comprises lipopolysaccharide and nigericin, gramicidin, a bacterial toxin, a reactive oxygen species (ROS), lipopolysaccharide and adenosinetriphosphate (ATP), polyphyllin VI, 6,7-dichloro-2-methylsulfonyl-3-N-tert-butylaminoquinoxaline (DMB), photodynamic therapy (PDT), or a combination thereof.

[0022] As described herein, lipopolysaccharide and nigericin successfully trigger pyroptosis of tumor cells. Gramidicin, a peptide antibiotic, damages cell membranes and can trigger pyroptosis. Bacterial toxins can form pores (e.g., Staphylococcal α-toxin, cytolysin A, hemolysin BL, and the like) and can trigger pyroptosis. Similarly, reactive oxygen species such as hydroperoxide, superoxide, hydroxyl radicals, and singlet oxygen damage cell membranes and can cause pyroptosis. Additional pyroptosis-inducing agents include lipopolysaccharide and adenosinetriphosphate (ATP), polyphyllin VI, and 6,7-dichloro-2-methylsulfonyl-3-N-tert-butylaminoquinoxaline (DMB) which stimulate pathways that activate the inflammasome. Photodynamic therapy (PDT) targeting mitochondria and endoplasmic reticulum can also stimulate pyroptosis.

[0023] In an aspect, prior to isolating the pyosomes, the method can further comprise imaging the treated tumor cells to verify a pyroptosis morphology, to verify pyosomes protruding from or excreted from the cell surface, or a combination thereof. Exemplary imaging techniques include scanning electron microscopy, confocal microscopy, or a

combination thereof. Pyrotopic cells have a unique morphology which can readily be identified using standard imaging techniques.

[0024] In an aspect, the pyosomes can be isolated using techniques for isolating EVs such as gradient centrifugation, size-based isolation, microfluidic isolation, membrane affinity spin columns (e.g., Qiagen® exoEasy Maxi Spin Columns), and combinations thereof.

[0025] In an aspect, the diameters, e.g., the median diameters) of the isolated pyosomes are distributed between 100 nm and 1000 nm. In general, the pyosomes had an average diameter (d50 based on dynamic light scattering) of about 278 nm which is larger than exosomes which have an average diameter of about 145 nm.

[0026] In an aspect, the isolated pyosomes have a zeta potential of about -8 mv. Exosomes in contrast have a zeta potential of -11 mv.

[0027] In another aspect, the isolated pyosomes comprise more than 2000 different types of proteins as determined by proteomic analysis. There were 1137 types of proteins shared between the tumor pyosomes and exosomes, however, there are over 1300 types of tumor-related proteins unique to the tumor pyosomes. In addition, the isolated pyosome express higher levels of key immunogenic damage-associated molecular patterns (DAMPs) such as high mobility group box 1 protein (HMGB1), heat shock protein 70 (HSP70), and calreticulin compared to tumor exosomes. As used herein, tumor exosomes are defined as membrane-bound vesicles released by tumor cells in the absence of pyroptosis-inducing agents.

[0028] In an aspect, the isolated pyosomes have an average diameter (d50 based on dynamic light scattering) of about 278 nm, a zeta potential of about -8 mv, and comprise more than 2000 proteins as discussed above.

[0029] In another aspect, the isolated pyosomes express elevated levels of microRNAs expressed in AMPK and PI3K-Akt signaling pathways (e.g., miR-203a, miR-125b, miR-103a-3p, miR-4299, miR-496, miR-107, miR-21) compared to tumor exosomes.

[0030] Also included is the product of the process described herein, i.e., a pyosome.

[0031] Also described herein are immunostimulant compositions comprising the pyosomes loaded with an immunostimulant.

[0032] Exemplary immunostimulants for loading into the pyosomes include resiquimod, imiquimod, gardiquimod, ODN 2395 sodium (SEQ ID NO: 2; 5'-tcgtcgttttcggcgc:gcgccg-3'), agatolimod, diprovocim, telratolimod, motolimod, vesatolimod, polyinosinic-polycytidylic acid sodium, paclitaxel, adriamycin, levamisole, a small molecule

immune checkpoint inhibitor (ICI) (BMS-200, BMS-202, CA-170, YPD-30, YPB-29B, INCB086550, MAX-10181), or a combination thereof. In an aspect, the immunostimulant is a compound not found in nature.

[0033] Also included are pharmaceutical compositions comprising the pyosomes loaded with an immunostimulant and a pharmaceutical carrier or excipient.

[0034] Exemplary pharmaceutical compositions include compositions suitable for implantation at the site of a solid tumor, particularly after surgical removal of a tumor.

[0035] In an aspect, the pharmaceutical composition comprises the immunostimulant pyosome suspended in a polymeric carrier such as a hydrogel. The composition may be an injectable or an implantable composition.

[0036] A hydrogel is a substance formed when an organic polymer (natural or synthetic) is cross-linked via covalent, ionic, or hydrogen bonds to create a three-dimensional open-lattice structure that entraps water molecules to form a gel. "Biocompatible hydrogel" refers to a hydrogel that is not toxic to living cells. In an aspect, the hydrogel comprises a synthetic, e.g., non-natural, organic polymer.

[0037] Examples of materials that can be used to form a biocompatible hydrogel include polysaccharides such as alginate, polyphosphazines, poly(acrylic acids), poly(methacrylic acids), poly(alkylene oxides), poly(vinyl acetate), polyvinylpyrrolidone (PVP), and copolymers and blends. Additional materials for forming hydrogels include agarose, alginic acid, chitosan, dextran, dextran sulfate, heparan, heparan sulfate, cellulose sulphate, carrageenan, gellan gum, xanthan gum, guar gum, chondroitin sulfate, hyaluronic acid, collagen, gelatin, hydroxyethyl starch, and poly(N-isopropyl acrylamide). Combinations of the foregoing materials may be employed.

[0038] In an aspect, the hydrogel is a thermosensitive hydrogel. Exemplary materials to form thermosensitive hydrogels include polyoxyethylene-polyoxypropylene (PEO-PPO) block copolymers such as Pluronic® F127 and F108, which are PEO-PPO block copolymers with molecular weights of 12,600 and 14,600, respectively. Each of these compounds is available from BASF (Mount Olive, N.J.). Pluronic® F108 can form a thermosensitive hydrogel at a concentration of 20-28% in phosphate buffered saline (PBS). Pluronic® F127 at a 20-35% concentration in PBS also forms thermosensitive hydrogels. When the hydrogel is a thermosensitive hydrogel, the composition can be in the form of a hydrogel patch. Advantageously, hydrogel patches can be implanted or placed adjacent to a solid tumor or surgical site to stimulate pyroptosis and treat cancer.

[0039] In another aspect, the hydrogel is an injectable hydrogel. Injectable hydrogels can include polysaccharides such as heparan, heparan sulfate, chitosan, hyaluronic acid, dextran, alginic acid and hydroxyethyl starch. A crosslinker such as a reactive polyethylene glycol crosslinker can be used to form the hydrogel. An exemplary injectable hydrogel is a hyaluronic acid hydrogel, formed by adding Extralink®-Lite (polyethylene glycol diacrylate (PEGDA)) was added to a Glycosil® (thiol-modified hyaluronan). Injectable hydrogels are locally injectable to release therapeutic agents at the site of a solid tumor.

[0040] In an aspect, a method of treating a patient in need of treatment for a solid tumor comprises administering to the patient the composition comprising the immunostimulant-loaded pyosomes.

[0041] In an aspect, the patient is in need of treatment for post-surgical tumor recurrence after removal of the solid tumor.

[0042] In an aspect, a method of treating a patient in need of treatment for post-surgical tumor recurrence comprises administering to the patient the injectable or implantable composition comprising an immunostimulant-loaded pyosome suspended in a polymeric carrier. The method can comprise locally injecting or implanting the injectable or implantable composition at the surgical site. In another aspect, the method comprises locally injecting or implanting the injectable or implantable composition at or near a lymph node.

[0043] In the foregoing aspects, the pyosomes may be isolated from a tumor removed from the patient.

[0044] In an aspect, the method further comprises administering a chemotherapeutic agent, a radiotherapeutic agent, or a combination thereof.

[0045] Non-limiting examples of chemotherapeutic agents include platinum-based drugs (e.g., oxaliplatin, cisplatin, carboplatin, spiroplatin, iproplatin, satraplatin, etc.), alkylating agents (e.g., cyclophosphamide, ifosfamide, chlorambucil, busulfan, melphalan, mechlorethamine, uramustine, thiotepa, nitrosoureas, etc.), anti-metabolites (e.g., 5-fluorouracil, azathioprine, 6-mercaptopurine, methotrexate, leucovorin, capecitabine, cytarabine, floxuridine, fludarabine, gemcitabine, pemetrexed, raltitrexed, etc.), plant alkaloids (e.g., vincristine, vinblastine, vinorelbine, vindesine, podophyllotoxin, paclitaxel, docetaxel, etc.), topoisomerase inhibitors (e.g., irinotecan, topotecan, amsacrine, etoposide (VP16), etoposide phosphate, teniposide, etc.), antitumor antibiotics (e.g., doxorubicin, adriamycin, daunorubicin, epirubicin, actinomycin, bleomycin, mitomycin, mitoxantrone, plicamycin, etc.), pharmaceutically acceptable salts thereof, stereoisomers thereof, derivatives thereof, analogs thereof, and combinations thereof.

[0046] Radiotherapeutic agents are well known in the art and can comprise external-beam radiation therapy and/or internal radiation therapy. External beam radiation therapy delivers radioactive beams of high energy X-rays and/or gamma rays to a patient's tumor, whereas internal radiation therapy delivers radioactive atoms to a patient's tumor. Both external beam radiation therapy and internal radiation therapy are used to suppress tumor growth or kill cancer cells by delivering a sufficient quantity of radioactivity to the target site. In some embodiments, the radiotherapeutic agent comprises a radioactive atom and is complexed with a biologic or synthetic agent to increase delivery to the target site. Such biologic or synthetic agents are known in the art. Exemplary radioactive atoms include any of the radionuclides described herein, or any other isotope which emits enough energy to destroy a targeted tissue or cell. In some embodiments, radiotherapeutic agents may be coupled to targeting moieties, such as antibodies, to improve the localization of radiotherapeutic agents to cancerous cells.

[0047] The term "radionuclide" is intended to include any nuclide that exhibits radioactivity. A "nuclide" refers to a type of atom specified by its atomic number, atomic mass, and energy state, such as carbon 14 (^{14}C). "Radioactivity" refers to the radiation, including alpha particles, beta particles, nucleons, electrons, positrons, neutrinos, and gamma rays, emitted by a radioactive substance. Examples of radionuclides include, but are not limited to, fluorine 18 (^{18}F), fluorine 19 (^{19}F), phosphorus 32 (^{32}P), scandium 47 (^{47}Sc), cobalt 55 (^{55}Co), copper 60 (^{60}Cu), copper 61 (^{61}Cu), copper 62 (^{62}Cu), copper 64 (^{64}Cu), gallium 66 (^{66}Ga), copper 67 (^{67}Cu), gallium 67 (^{67}Ga), gallium 68 (^{68}Ga), rubidium 82 (^{82}Rb), yttrium 86 (^{86}Y), yttrium 87 (^{87}Y), strontium 89 (^{89}Sr), yttrium 90 (^{90}Y), rhodium 105 (^{105}Rh), silver 111 (^{111}Ag), indium 111 ($_{111}In$), iodine 124 (^{124}I), iodine 125 (^{125}I), iodine 131 (^{131}I), tin 117m (^{117m}Sn), technetium 99m (^{99m}Tc), promethium 149 (^{149}Pm), samarium 153 (^{153}Sm), holmium 166 (^{166}Ho), lutetium 177 (^{177}Lu), rhenium 186 (^{186}Re), rhenium 188 (^{186}Re), thallium 201 (^{201}Tl), astatine 211 (^{211}At), and bismuth 212 (^{212}Bi). As used herein, the "m" in ^{117m}Sn and ^{99m}Tc stands for the meta state. Additionally, naturally-occurring radioactive elements such as uranium, radium, and thorium, which typically represent mixtures of radioisotopes, are suitable examples of radionuclides. ^{67}Cu, ^{131}I, ^{177}Lu, and ^{186}Re are beta- and gamma-emitting radionuclides. ^{221}Bi is an alpha- and beta-emitting radionuclide. ^{211}At is an alpha-emitting radionuclide. ^{32}P, ^{47}Sc, ^{89}Sr, ^{90}Y, ^{15}Rh, ^{111}Ag, ^{117m}Sn, ^{149}Pm, ^{153}Sm, ^{166}Ho, and ^{186}Re are examples of beta-emitting radionuclides. ^{67}Ga, ^{111}In, ^{99m}Tc, and ^{201}Tl are examples of gamma-emitting radionuclides. ^{55}Co, ^{60}Cu, ^{61}Cu, ^{62}Cu, ^{66}Ga, ^{68}Ga, ^{82}Rb, and ^{86}Y are

examples of positron-emitting radionuclides. ^{64}Cu is a beta- and positron-emitting radionuclide.

[0048] The invention is further illustrated by the following non-limiting examples.

Examples

Methods

[0049] Cell lines and antibodies: The murine 4T1, B16F10, MC38 cell lines, and human MDA-MB-231 cell lines were purchased from ATCC. 4T1-Luc and B16F10-OVA cell lines were purchased from Vitro Biotech. Cells were cultured in the CO_2 incubator (Fisher) at 37°C with 5% CO_2 and 90% relative humidity. The antibodies used in this study were summarized as follows (company, clone, category number): GoInVivo™ Purified anti-mouse CD279 (PD-1) (BioLegend, RMP1-14, 114114), fluorescein isothiocyanate (FITC)-anti-mouse CD45 (BioLegend, 30-F11, 103108), APC-anti-mouse CD3 (BioLegend, 17A2, 100236), FITC-anti-mouse CD4 (BioLegend, GK1.5, 100406), PE-anti-mouse CD8a (BioLegend, 53-6.7, 100708), FITC-anti-mouse IFNγ (BioLegend, XMG1.2, 505806), PerCP/Cy5.5-anti-human/mouse Granzyme B (Bioligands, QA16A02, 372212), PE-anti-mouse CD45 (BioLegend, 30-F11, 103106), Alexa Fluor® 594 anti-mouse CD8a (BioLegend, 53-6.7, 100758), FITC-anti-mouse CD11c (BioLegend, N418, 117306), PE-anti-mouse CD80 (BioLegend, 16-10A1, 104708), APC-anti-mouse CD86 (BioLegend, GL-1, 105012), PE anti-mouse H-2Kb bound to SIINFEKL (SEQ ID NO: 1) Antibody (BioLegend, 25-D1.16, 141603), Precision Count Beads (BioLegend, 424902). Mouse Reactive Pyroptosis Antibody Sampler Kit (Cell Signaling Technology, 98303T), HRP Anti-beta Actin antibody (Abcam, ab49900). All antibody dilutions were performed following the manufacturer's guidance (for flow cytometry assay: diluted by approximately 200 times for use; for Western Blot assay: antibodies from Cell Signaling Technology diluted by approximately 1,000 times for use; HRP Anti-beta Actin antibody from Abcam: diluted by approximately 10,000 times for use).

[0050] Extraction and characterization of pyosomes: To isolate pyosomes, 4T1, B16F10, MC38, and MDA-MB-231 cells were cultured in 6-well plates and treated with lipopolysaccharide (LPS) with a concentration of 1 μg/ml in PBS, 1 ml per well. After a 3-hour incubation at 37°C, nigericin (abbreviated Nig) was added to the wells at concentrations of 10 μM and incubated for an additional 50 min. Then cells were pipetted with PBS, and the suspension was collected and centrifuged at 300 g for 10 min to remove cells at 4°C. The supernatant was centrifuged at 3,000 g for 20 min. Afterward, the supernatant was collected

and further centrifuged at 12,000 g for 30 min to pellet the pyosomes, which were then resuspended in 1ml PBS.

[0051] To collect tumor cell exosomes, the supernatant from untreated cells was centrifuged at 2,000 g for 20 min to remove cells. The suspension was centrifuged at 10,000 g for 30 min. Then, the supernatant was collected and centrifuged at 100,000 g for 120 min to pellet the exosomes, which were then resuspended in 1ml PBS.

[0052] The untreated and LPS+Nig-treated cells were stained with WGA-Rhodamine B and Hoechst 33342 and washed with PBS before confocal imaging. The morphology of the cells and pyosomes were observed under SEM (Zeiss Gemini 450 FESEM). The pyosomes were subjected to TEM analysis (FEI Tecnai T-12 Cryo TEM system). Then, the size and zeta potential of pyosomes were measured using a Malvern Zetasizer instrument.

[0053] Lactate dehydrogenase (LDH) release assay: To detect LDH release from tumor cells, cells were seeded in a 96-well plate in triplicate, incubated overnight, and treated with PBS or LPS+Nig. Several controls were included: a complete media control without cells, a serum-free media control, spontaneous LDH activity controls, and maximum LDH activity controls. Sterile water was added to spontaneous controls. Lysis buffers were added to the maximum activity controls. Then 50 µl of each sample was transferred to a new plate, including all controls and compound-treated samples. After this, the reaction mixture was added to the wells. 30 min later, a stop solution was added. The absorbance at 680 nm was subtracted from the absorbance at 490 nm to determine LDH activity. The results were calculated based on the equation: LDH release% = (sample activity-spontaneous controls activity) / (maximum control activity-spontaneous controls activity) × 100.

[0054] PI and SYTOX™ Green staining assay: To assess propidium iodide (PI) and SYTOX™ Green cell uptake, 4T1 and B16F10 tumor cells were cultured in 6-well plates and treated with LPS+Nig as described above. After incubation, the cells were gently pipetted with PBS, and the cell suspension was collected. The cells were centrifuged at 1,200 rpm for 5 min, and the pellets were collected. PI and SYTOX™ Green staining were performed respectively according to the manufacturer's instructions. After staining, the cells were washed with PBS, resuspended in 500 µl PBS, and analyzed by flow cytometry.

[0055] Protein Extraction and Western Blot assay: 4T1 and B16F10 cells treated with PBS or LPS+Nig were first washed with PBS, followed by trypsinization and collection into 1.5 ml tubes. The samples were centrifuged at 1,000 rpm for 4 min to pellet the cells. Next, 100 µl of Pierce™ RIPA buffer with a protease inhibitor cocktail was added to each tube for cell lysis. After 1-hour lysis, the samples were centrifuged at 14,000 rpm for 30 min at 4°C

to collect the supernatant. Bicinchoninic acid assay (BCA) analysis was conducted to determine protein concentration. The samples were mixed with loading buffer, heated at 100°C for 15 min, and stored at 4°C.

[0056] In the Western Blot assay, protein samples with equal amounts of proteins and markers were carefully loaded onto a gel. The electrophoresis was conducted at 120 V until the bromophenol blue dye reached the end of the gel. Subsequently, proteins were transferred to a polyvinylidene fluoride (PVDF) membrane at 350 mA for 85 min. The membrane was then soaked in 5% non-fat dry milk for 2 hours at room temperature and incubated overnight at 4°C with primary rabbit antibodies targeting cleaved gasdermin D (GSDMD) and cleaved caspase-1. Following the primary antibody incubation, the membranes underwent three washes with TBST and were then incubated with an anti-rabbit IgG HRP-linked secondary antibody for 1 hour at room temperature. β-actin was tested by incubating the membrane with the HRP Anti-beta Actin antibody. After a final set of three TBST washes, Western Blot substrates were applied to the membranes, and the resultant images were captured using an iBright™ Imaging System.

[0057] Proteomics analysis: Liquid chromatography-tandem mass spectrometry (LC-MS/MS) analysis was performed at the Mass Spectrometry Facility, the Analytical Instrumentation Center (AIC) of the University of Wisconsin School of Pharmacy. To prepare proteomic samples, pyosomes and exosomes were extracted from 4T1 cells and resuspended in ammonium bicarbonate (ABC) solutions (100 mM) on ice. The samples were homogenized using a syringe with a 23-gauge needle by pulling back and depressing the plunger. The lysates were then centrifugated at 15,000 g for 20 min at 4°C, and the supernatants were collected. A bicinchoninic acid (BCA) assay was conducted to determine the concentration of the proteins. Then, samples containing 20 μg proteins were reduced with 10 mM DL-Dithiothreitol at 37°C for 30 min. Subsequently, an iodoacetamide solution was added to the samples (final concentration 55 mM) and incubated for another 45 min in the dark. The samples were digested in trypsin (0.1 g/L in 250 mM ABC solution) for 18 hours. The digestion was quenched with formic acid. The samples were dried in a speed vacuum concentrator.

[0058] The LC separations were conducted using a Waters NanoACQUITY UPLC. The peptide solutions were reconstituted in 0.1% formic acid solution and sampled onto the column. Mobile phases A (water with 0.1% formic acid) and B (acetonitrile with 0.1% formic acid) were used to develop a gradient elution (0.350 μl/min). The gradient was set as follows: from 0 to 1 min, B increased from 3% to 5%, followed by an increase to 30% at 110

min; at 115 min, the column was washed with 95% B; then 95% B was maintained for another 10 min. Then, B ramped back to 3% in 3 min, and the column was re-equilibrated for 10 min. An Orbitrap Q-Exactive™ MS (Thermo Fisher Scientific) was used for analysis. The instrument was operated at positive ion mode with nano-ESI high-resolution Q-Exactive™ analysis. The full MS scan resolution was set to 70,000 resolutions with an automated gain control (AGC) target value of 10^6 in the range of 300-2,000 m/z and a max injection time of 100 ms. Then, a Microscan was acquired at a resolution of 17,500 with an AGC target of 10^5, a dynamic exclusion of 7 s, a 3.5 m/z isolation window, a max injection time of 100 ms, a loop count of 10, and a normalized collision energy of 30.

[0059] MicroRNA sequencing: Three replicates from pyosomes and exosomes were submitted to the Gene Expression Center of the University of Wisconsin for small RNA sample preparation and analysis. The microRNA libraries were prepared using a QIASeq® miRNA Library Kit (Qiagen, Netherlands). Then, quality control and Next Generation Sequencing (NGS) were performed. Libraries were sequenced on an Illumina® NovaSeq™ X Plus platform. Then, base calling was performed using Illumina®'s CASAVA. The obtained raw data was filtered and quality-trimmed to obtain clean data. Next, the reads were aligned to miRBase mature microRNA reference using BLAST to identify known microRNAs. The sequences that did not match the known miRNAs and non-coding RNA in GenBank were used for novel miRNA prediction.

[0060] Preparation of resiquimod-loaded pyosomes and vaccine gel: Pyosomes (1 μg/ml) were incubated with resiquimod (100 ng/ml) at 37°C for 6 h. Afterward, the mixture was collected and further centrifuged at 12,000 g for 30 min to pellet the resiquimod-loaded pyosomes, which were then resuspended in 1ml PBS. To prepare Pyo-R@Gel and Pyo@Gel vaccines, the pyosomes with or without resiquimod were loaded into a thiol-modified hyaluronic acid hydrogel (Advanced BioMatrix, GS1004) following the manufacturer's guidance.

[0061] Bone marrow derived dendritic cell (BMDC) extraction and in vitro immune assay: To isolate and culture BMDCs, the mouse legs were cut above the hip joint to harvest the intact femur and tibia. Muscle and tissue were carefully debrided without breaking the bones. The bones were then immersed in sterilized PBS with Penicillin-Streptomycin. The bones were rinsed in ethanol for 10 seconds before being transferred into a dish with culture media. The very ends of the bones were trimmed off, and 10 ml of media was used to flush the marrow from the bones. Bone fragments were filtered out using a cell strainer, and cells were pelleted by centrifugation at 1,000 rpm for 5 min. Red blood cells were lysed, and cells

were re-pelleted at 1,000 rpm for 5 min. The resulting cell pellet was resuspended in 10 ml of media and filtered again. Cells were then plated at a density of 1×10^6 cells per ml of media on a 10 cm petri dish using RPMI 1640 media supplemented with 10% heat-inactivated FBS. Recombinant GM-CSF at 20 ng/ml and IL-4 at 10 ng/ml were added to the culture. Half of the medium was changed every two days to allow the cells to expand and differentiate over 5 to 7 days. Afterward, the cells were passaged; BMDCs, which adhere loosely to the dish wall, were collected easily during pipetting with chilled PBS. After passage, BMDCs were cultured for 2 to 3 days to form suspending cell clusters. The cells were collected by gentle pipetting and centrifugation for further studies.

[0062] To investigate the impact of different treatments on BMDC maturation, the cells were treated with PBS, R, Exo, Pyo, Exo-R, and Pyo-R for 48 h. Then, the cells were collected by centrifugation, washed with PBS, and stained with PE-anti-mouse CD80 and APC-anti-mouse CD86 before the flow cytometry assay. The cell supernatants were also collected, and the levels of TNFα and IL-12p70 were measured using corresponding ELISA kits.

[0063] *In vivo* anti-tumor assay: To verify the anti-tumor efficacy *in vivo*, the 4T1-Luc orthotopic triple negative breast cancer (TNBC) model was established by implanting 4T1-Luc cells into the breast pad of the mice. When the tumor volume reached around 150 mm^3, surgical resection was performed under a microscope to remove the tumor mass as much as possible. Different treatments were applied to the tumor cavity, including blank Gel, Pyo@Gel, R@Gel, Pyo-R, Exo-R@Gel, and Pyo-R@Gel. The dose of resiquimod was 0.5 mg/kg, and doses of Pyo or Exo were 5 mg/kg. For the gel groups, the pyosomes or exosomes were loaded in 200 μl hydrogels before being injected into the tumor cavity. IVIS imaging was performed twice a week to monitor the tumor recurrence and metastasis. On day 21, four of the mice were euthanized and the lung tissues were harvested and stained with Bouin's solution. A hematoxylin and eosin (H&E) assay was performed by the UW-Madison Carbone Cancer Center Experimental Pathology Lab. The survival of the mice was monitored until Day 70. Mice were euthanized upon reaching any of the humane endpoints, including weight loss >20%, inability to ambulate, moribund and tumor volume >2000 mm^3. The tumor volume was calculated as length $\times$ $width^2 \times 0.5$.

[0064] The B16F10 double tumor model was established to verify the therapeutic efficacy of the pyosome vaccine. First, the primary tumor was established by injecting B16F10 tumor cells into the right flank of the mice on Day -10. On Day -1, B16F10 tumor cells were injected into the left flank of the mice as the second tumor. On Day 0, surgery was

performed to partially remove the primary tumor, and pyosome vaccine was implanted in the surgical bed. The growth of the second tumor was monitored by measuring the tumor site using a caliper every week. Survival of the mice was monitored until Day 60.

[0065] The humanized NeoThy mice (NSG mice with human immune system) were established by the UW Humanized Mouse Core. To establish the PDX model, patient TNBC tissues were cut into small pieces and implanted into the breast pads of the mice. Surgery was performed after 3 weeks of tumor injection to remove the tumor mass as much as possible. Pyosomes were extracted from the resected tumors and loaded into gels. The gels were implanted back into the post-surgical tumor cavity. Tumors were collected 4 weeks later, and tumor volume and weight were measured.

[0066] In vivo immune assay: 4T1, B16F10-OVA, and MC38 models were established, and different treatments including blank Gel, Pyo@Gel, R@Gel, Pyo-R, Exo-R@Gel, and Pyo-R@Gel were performed as mentioned above. To analyze immune cell composition by flow cytometry, tumors and lymph nodes were collected on Day 14. Each tumor is placed in 2 ml of media containing collagenase and disrupted using a homogenizer. The homogenized tissues were filtered through a cell strainer, and the cell suspension was centrifuged at 350 g for 8 min. The supernatant was collected for ELISA assay. The cell pellet was resuspended in PBS and washed once. The cells were then stained in the dark with the desired antibodies for one hour and then washed once with PBS. Lastly, the cells were resuspended in 500 ml PBS for flow cytometry analysis.

[0067] Biosafety evaluation of AST, ALT, and BUN: The serum of mice was collected 2 weeks after the implantation of the pyosome vaccine. Samples were prepared as per the specific requirements for each assay. Reagents included enzyme solutions, chromogenic agents, and other necessary buffers and solutions as provided in the respective test kits. In the AST and ALT assays, the enzymatic activity was determined using the AST Colorimetric Activity Assay Kit (Item No. 701640) and ALT Colorimetric Activity Assay Kit (Item No. 700260). The assays were based on the enzymatic conversion of specific substrates, leading to a colorimetric reaction. Absorbance was measured using a microplate reader at 340 nm, and enzyme activity was calculated based on the change in absorbance over time. BUN levels were measured using the Urea BUN Colorimetric Assay Kit (Catalog No: E-BC-K183-M) based on the Urease Method. The procedure involved the decomposition of urea into ammonia ions and carbon dioxide, followed by a colorimetric reaction. The absorbance was measured at 580 nm, and the urea content was quantified from a prepared standard curve.

[0068] Statistics: All the results are shown as mean ± s.d.. The GraphPad Prism software was used to perform statistical analysis. Unpaired Student-*t* test was used to compare two groups and analysis of variance (ANOVA) was used to compare multiple groups (> two groups) statistically. Log-rank test was performed for the statistical analysis of the survival study. A P value lower than 0.05 ($*P < 0.05$) was considered the threshold for statistical significance among control groups and experimental groups.

Example 1: Verification of pyosome formation

[0069] To induce pyroptosis of tumor cells, mouse 4T1 TNBC cells were treated with lipopolysaccharide (LPS) and nigericin (designated LPS+Nig). To validate if this method successfully triggered cell pyroptosis, cell morphologies were observed under a scanning electron microscope (SEM). Cells undergoing pyroptosis were characterized by typical morphological changes, such as swelling and large protrusions. Through SEM imaging, 4T1 cells treated with LPS+Nig displayed obvious pyroptosis morphology. Notably, in addition to changes in cell morphology, many spherical vesicle-like pyosomes were observed protruding from the cell surfaces (FIG. 1a), in which the size of the formed pyosomes was approximately distributed between 100 nm and 1000 nm. Further, the formation of pyosomes in 4T1 tumor cells was confirmed through confocal microscopy (FIG. 1b). Besides attaching to the cell surface, it was found that some of the produced pyosomes were secreted into the external microenvironment. In contrast to the normal 4T1 cells with a relatively smooth surface (FIGs. 1c, d), 4T1 cells treated with LPS+Nig displayed a distinct transformation to protruded vesicles on the membrane. To verify whether this finding was applicable to other tumor cells, B16F10 cells were treated with the same method and spherical pyosomes were also formed on the cell surface of B16F10 cells through SEM (FIGs. 1e, g) and confocal imaging (FIGs. 1f, h).

Example 2: Extraction and characterization of pyosomes

[0070] Having validated the generation of vesicles in LPS+Nig-treated cells, cell pyroptosis was characterized and pyosomes were extracted as illustrated in FIG. 2a. First, the lactate dehydrogenase (LDH) release in tumor cells treated with LPS+Nig was detected to assess the membrane rupture in pyroptotic cells. Compared to untreated cells with minimal LDH release, nearly 40% of LDH was released to the extracellular environment in 4T1 cells (FIG. 3b) and nearly 60% of LDH was released in B16F10 cells (FIG. 2c). Pyroptosis is reported to be accompanied by pore formation and loss of membrane integrity, which can be

probed by SYTOX™ Green and PI staining. As shown in FIGs. 2d-g, significant cellular uptake of SYTOX™ Green and PI was observed through flow cytometry assay in both LPS+Nig-treated 4T1 (FIGs. 2c, 2d) and B16F10 cells (FIGs. 2f, 2g). Since the cell pyroptosis is mechanistically triggered by activated caspase proteins that will subsequently cleave gasdermin family proteins to induce cell swelling and membrane rupture, a Western Blot assay was performed to validate the activation of caspase and gasdermin proteins in the pyroptosis signaling pathway. As shown in FIGs. 2h, i, the LPS+Nig treatment could result in both cleaved caspase-1 and activated gasdermin D (GSDMD) proteins to trigger tumor pyroptosis of 4T1 cells (FIG. 2h) and B16F10 cells (FIG. 2i).

[0071] Next, the pyosomes were extracted from the pyroptotic tumor cells through a gradient centrifugation method, which is frequently used in isolating tumor-derived EVs. As shown in FIG. 2j, the extracted pyosomes displayed a uniform distribution with an average size (D50 determined by dynamic light scattering) of around 278 nm. The pyosomes extracted from different tumor cells did not show significant differences in size (FIG. 2k). In addition, SEM revealed spherical structures of the extracted pyosomes (FIG 2l), corroborated by TEM imaging, which showed spherical structures resembling cellular vesicles (FIG. 2m). The extracted pyosomes from both 4T1 and B16F10 cells exhibited a similar zeta potential of around -8 mv (FIG. 2n). To compare the physicochemical properties and functions of pyosomes with other EVs, exosomes from 4T1 and B16F10 cells were also extracted. Exosomes displayed an average size of around 145 nm and a zeta potential of -11 mv (data not shown).

Example 3: Protein and microRNA analysis of the pyosomes

[0072] After the basic characterization of the extracted tumor cell pyosomes, the content of pyosomes was explored, with a particular interest in the protein and microRNA composition, which is critical to determine their immunogenicity. Proteomic analysis of the pyosomes (designated Pyo) from 4T1 cells was performed and there was a rich variety of proteins, with more than 2000 types detected, which is significantly higher than the exosomes (designated Exo) extracted from the same batch of normal 4T1 tumor cells (FIG. 3a). There were 1137 types of proteins shared between the tumor pyosomes and exosomes, and there are over 1300 types of tumor-related proteins unique to the tumor pyosomes (FIG. 3a). Moreover, the quantity and content of inflammatory proteins (such as HMGB1, HSP70, calreticulin) in the pyosomes were significantly higher than those in the tumor exosomes, which is in line with the feature of pyroptosis as a type of inflammatory cancer cell death

(FIGs. 3b-c). In addition, some tumor antigens, such as Erbb2 and Msln, were also found on the pyosomes and exosomes. Equipped with these immune-stimulating inflammatory factors and preserved tumor-associated antigens, pyosomes are expected to exhibit strong immunogenicity and have great potential to serve as tumor vaccine platforms.

[0073] Next, microRNA gene analysis was performed on the tumor pyosomes. The microRNA profiles in the tumor pyosomes and exosomes are remarkably different, which displayed 203 differentially expressed microRNAs, with 170 microRNAs downregulated and 33 microRNAs upregulated (FIG. 3d). In these differential microRNA expressions, the particular microRNAs that have been validated to closely related to tumor pyroptosis triggered by NLRP3 inflammasome were identified, as shown in FIG. 3e. A Kyoto Encyclopedia of Genes and Genomes (KEGG) analysis revealed that the inflammatory programmed cell death pathways were enriched in the differentially expressed microRNAs, including AMPK and PI3K-Akt signaling pathways that can activate NLRP3 inflammasome to trigger tumor pyroptosis (FIG. 3f). Collectively, these mechanistic studies revealed the critical biomolecular components determining the strong immunogenicity of pyosomes.

Example 4: Anti-tumor recurrence efficacy of pyosome vaccines in post-surgical metastatic TNBC and melanoma mouse models

[0074] To validate the vaccination efficacy of pyosomes in preventing post-surgical tumor recurrence, tumor models with a high probability of recurrence after surgery in the clinic, such as TNBC and aggressive melanoma, were established. Here, an immunostimulant resiquimod was encapsulated into the pyosomes (designated Pyo-R) to enhance the dendritic cell (DC) activation and maturation. About 20% loading efficiency of resiquimod in the pyosomes was achieved through the co-incubation method. To facilitate the *in vivo* implementation and improve the local retention of the Pyo-R at the tumor site, the Pyo-R was loaded into a biocompatible HA hydrogel (designated Pyo-R@Gel) which can be implanted in the post-surgical tumor cavity.

[0075] Afterward, a 4T1-Luc TNBC recurrence model was established, in which Pyo-R@Gel was implanted into the post-surgical tumor cavity after the removal of the tumor mass as much as possible under a microscope. Here, exosomes from 4T1-Luc cells were also collected and engineered to encapsulate resiquimod and further loaded into the HA hydrogel to construct Exo-R@Gel for the head-to-head comparison with Pyo-R@Gel. The post-surgical 4T1 TNBC-bearing mice were treated with various groups including: (1) blank HA hydrogel (Gel); (2) pyosomes-loaded HA hydrogel (Pyo@Gel); (3) resiquimod-loaded HA

hydrogel (R@Gel); (4) resiquimod-loaded pyosomes (Pyo-R); (5) resiquimod-loaded exosomes embedded in HA hydrogel (Exo-R@Gel); (6) resiquimod-loaded pyosomes embedded in HA hydrogel (Pyo-R@Gel). The growth and recurrence of tumors, represented by the bioluminescence signals from 4T1-Luc cells, after different treatments were monitored by In Vivo Imaging Systems (IVIS) imaging. Encouragingly, the Pyo-R@Gel group effectively inhibited tumor recurrence, outperforming the Exo-R@Gel group, as evidenced by the weaker bioluminescence signals of 4T1-Luc tumors throughout the treatment course (FIG. 4a). Moreover, the Pyo-R@Gel extended the median survival of the post-surgical 4T1-Luc tumor-bearing mice from 26 days (blank Gel group) to 68.5 days, which is significantly longer than the Exo-R@Gel (49 days), highlighting the unique advantages of pyosomes over exosomes as the vaccine platform (FIG. 4b). Pyo-R@Gel also contributed to a better survival benefit than Pyo-R (median survival: 45.5 days), presumably due to the better local retention of the pyosomes in the hydrogel within tumor sites. In comparison, Pyo@Gel and R@Gel only exerted moderate therapeutic effects, substantiating the enhanced efficacy of the combination of pyosomes and immunostimulants.

[0076] To further investigate if this local Pyo-R@Gel vaccine could elicit a systemic immune response to inhibit breast cancer metastasis, which is one of the major reasons for the dismal treatment efficacy of TNBC in the clinic. As shown in FIG. 4c, the Pyo-R@Gel vaccine remarkably inhibited the lung metastasis of 4T1 TNBC, demonstrated by the reduced number of tumor metastatic foci in the lungs compared to Exo-R@Gel and Pyo-R groups. In addition, lung tissue images (FIG. 4d) and H&E staining (FIG. 4e) both visually validated that the Pyo-R@Gel group could substantially reduce the number and size of tumor metastatic foci that spread to the lung tissues. Collectively, these results substantiated the superiority of pyosomes over exosomes as a vaccine platform in triggering both local and systemic immune responses to prevent tumor recurrence and metastasis.

[0077] To further verify the anti-tumor effect of the Pyo-R@Gel vaccine on a different tumor model, a B16F10 melanoma double-tumor model was established, as illustrated in FIG. 4f. After surgery on the primary tumor site, the Pyo-R@Gel was implanted into the post-surgical cavity, and the growth of the distant tumor was monitored by measuring the tumor site. As shown in FIG. 4g, Pyo-R@Gel vaccine could inhibit the growth of untreated distant tumors, with efficacy markedly superior to other treatment groups. On Day 21, the average tumor volumes in the Pyo-R@Gel group were 131 mm^3, significantly smaller than those in blank Gel (1714 mm^3, 13-fold decrease) and Exo-R@Gel (550 mm^3, 4.2-fold decrease) (FIG. 4f). Moreover, the Pyo-R@Gel extended the median

survival of the post-surgical B16F10 melanoma double tumor-bearing mice from 25.5 days (blank Gel group) to 57 days, which is significantly longer than the Exo-R@Gel (40.5 days) (FIG. 4h).

[0078] The biosafety profile of the Pyo-R@Gel vaccine was examined *in vivo*. The serum levels of alanine aminotransferase (ALT) and aspartate aminotransferase (AST), indicators for liver function damage, did not change significantly in the Pyo-R@Gel group compared to those in blank gel-treated mice. (data not shown) In addition, serum levels of blood urea nitrogen (BUN), an indicator of kidney function, were also similar in Pyo-R@Gel and blank gel groups.

Example 5: Immune activation of pyosome vaccines

[0079] After verifying the anti-tumor activity in vivo, the immune activation capability of pyosome vaccines was explored. Immune stimulation of pyosome vaccines on bone marrow-derived dendritic cells (BMDCs) was studied. Pyo-R treatment effectively promoted the maturation of DC cells, as evidenced by increased expression of CD80 on the surface of DC cells from 20.8% (PBS group) to 59.6%, and CD86 from 23.1% (PBS group) to 66.0%, significantly higher than those in the Exo-R group (CD80: 39.6%, CD86: 42.0%) (FIGs. 5a-d). Moreover, after stimulation by Pyo-R vaccines, the secretion of cytokines by DC cells increased significantly, with a 1.6-fold increase in TNFα level and a 1.8-fold increase in IL-12p70 level compared with the Exo-R group (FIGs. 5e, f).

[0080] To validate the immune activation capability of the Pyo-R vaccine *in vivo*, a 4T1 tumor recurrence mouse model with local implantation of Pyo-R@Gel into the post-surgical tumor cavity was established. On day 14 post-treatment, lymph nodes and tumor tissues were collected for the different treatments to study the activation of DC cells and T cells. The Pyo-R@Gel group increased the maturation rate of DC cells, evidenced by the increase in $CD80^+CD86^+$ DC cell populations, from 18.1% (blank Gel) to 48.1%, significantly higher than those in the Exo-R@Gel (33.0%, 1.5-fold increase) treatment group (FIG. 5g). In addition, T cell infiltration in tumor tissues after vaccination was analyzed. Flow cytometry results showed that the Pyo-R@Gel group increased the infiltration of $CD8^+$ T cells from 15.7% (blank Gel) to 54.3%, which is 1.6-fold and 1.8-fold higher than the Pyo-R and the Exo-R@Gel groups (FIG. 5h), respectively. In addition, significantly elevated cytokine levels of IFNγ and TNFα were detected after the treatment of Pyo-R@Gel, as

shown by a 5.2-fold increase in IFNγ and a 6.9-fold increase in TNFα levels in the tumor tissues compared with the blank gel group.

Example 6: Antigen-specific immune activation of pyosome vaccines

[0081] To demonstrate the antigen-specific immune response induced by the pyosome vaccine, ovalbumin (OVA) was selected as a model antigen and pyosomes were constructed from OVA-expressing B16F10 tumor cells. After surgery on the OVA-B16F10 tumors and implantation of the OVA-Pyo-R@Gel, the tumors were collected on day 14 post-treatment and analyzed for the expression of H-2K^b (SIINFEKL; SEQ ID NO: 1) on the surface of DC cells and the population of Tetramer$^+$CD8$^+$ T cells. It was found that pyosome vaccine could specifically increase the expression of H-2K^b (SIINFEKL) on the surface of DC cells, with its expression level rising from 1.6% in the blank Gel group to 31.6%, significantly higher than the Pyo-R group (19.3%, 1.6-fold increase) and the Exo-R@Gel group (19.9%, 1.6-fold increase) (FIGs. 6a, 6c). To study the antigen-specific activation of T cells, the Tetramer targeting the SIINFEKL; SEQ ID NO: 1 and found that after stimulation with the Pyo-R@Gel, the expression of the specific receptor against SIINFEKL on T cells increased from 2.5% in the blank Gel group to 26.8%, significantly higher than Pyo-R (14.8%, 1.8-fold increase) and Exo-R@Gel (15.8%, 1.7-fold increase) (FIGs. 6b, 6d).

[0082] To further demonstrate the capability of the pyosome vaccine against neoantigens, the reported neoantigen in MC38 colon tumor cells with a single-epitope mutation in Adpgk protein, which is presented in H-2D^b protein, was targeted. On a post-surgical MC38 tumor-bearing mouse model, the induction of antigen-specific CD8$^+$ T cell responses in both blood and tumors were tested by Adpgk Tetramer staining. The Pyo-R@Gel increased the Tetramer$^+$CD8$^+$ antigen-specific T cell populations in the blood from 2.1% (blank Gel group) to 19.6%, significantly higher than the Pyo-R group (11.3%, 1.7-fold increase) and Exo-R@Gel group (11.2%, 1.8-fold increase) (FIG. 6e, 6g). In tumor tissues, the antigen-specific activation of CD8$^+$ T cells from 1.8% (blank Gel group) to 22.0% (Pyo-R@Gel), proving the excellent CD8$^+$ T cell activation ability of the pyosome vaccines (FIG. 6f, 6h). Moreover, Pyo-R@Gel elicited 2-fold greater frequencies of antigen-specific CD8$^+$ T cells than Exo-R@Gel, demonstrating the better immune stimulation efficacy of pyosomes over exosomes. Collectively, these results validated that the pyosome vaccine elicited potent antigen-specific immune responses.

Example 7: Therapeutic efficacy of pyosome vaccines in humanized PDX mouse model

[0083] Before evaluating the vaccination efficacy of pyosomes on a humanized PDX mouse model, the generation and extraction of pyosomes from human cancer cells was validated. Human TNBC MDA-MB-231 cells treated with LPS+Nig exhibited typical features of pyroptosis, in which their morphology was significantly different from that of normal MDA-MB-231 (FIG. 7a). Flow cytometry analysis with SYTOX^{TM} Green and PI corroborated the pyroptotic state of the MDA-MB-231 cells (FIGs. 7b, 7c). In addition, the generation of pyosomes was observed in the MDA-MB-231 cells undergoing pyroptosis. The produced pyosomes from MDA-MB-231 cells were collected with an average size of 295 nm (FIG. 7d).

[0084] To further assess the clinical translation potential of pyosome vaccines, the anti-tumor recurrence activity was tested on a PDX TNBC-bearing humanized mouse model. The human immune system was implanted into NOD scid gamma (NSG) mice to construct a humanized mouse model (FIG. 7e). Afterward, TNBC tumor tissues were collected from clinical patients and established a PDX TNBC-bearing humanized mouse model. Once the tumor grew to a certain size, the tumor mass was surgically removed as much as possible under a microscope to mimic the clinical TNBC surgery treatment. The resected tumors were used to generate a personalized pyosome vaccine, which was loaded into the HA hydrogel and further implanted into the post-surgical tumor cavity of the corresponding mouse. The tumors were collected 4 weeks after the treatment. The average tumor volumes in the Pyo-R@Gel group were 55 mm^3, significantly smaller than those in blank Gel (610 mm^3, 11.1-fold decrease) and Exo-R@Gel (272 mm^3, 4.9-fold decrease) (FIGs. 7f, 7g). The average tumor weight in the Pyo-R@Gel vaccine group (75 mg) was also lower than that in the blank Gel group (630 mg, 8.4-fold decrease) and Exo-R@Gel group (238 mg, 3.2-fold decrease), demonstrating superior efficacy in inhibiting tumor recurrence and growth (FIG. 7h). These data highlighted the personalized pyosome vaccines could effectively prevent post-surgical patient-derived tumor recurrence by eliciting the tumor-specific immune response, further paving the way for the future clinical translation.

Discussion

[0085] Tumor vaccines that aim to cultivate the body's immune system to recognize and eliminate cancer cells have opened a new way for precision medicine to combat malignant tumors. With the capabilities to induce robust, tumor-specific, and long-term immunity, they have been envisioned as a promising strategy to prevent tumor recurrence after surgery. However, most tumor vaccines failed to show favorable anti-tumor therapeutic

outcomes despite eliciting antigen-specific T-cell immune responses. Particularly, traditional vaccines targeting a single antigen are difficult to induce strong tumor-specific T cell response even with extensive antigen modifications and optimizations due to (1) tumor antigen heterogeneity, (2) patient individual differences, and (3) suboptimal immunogenicity, highlighting the critical need to develop personalized tumor vaccine that can be tailored for the individual patient.

[0086] In this study, pyosomes were discovered, a new type of tumor EVs produced during the pyroptosis process of tumor cells, their potential as a personalized tumor vaccine was substantiated (FIG. 8). The pyosomes generated during pyroptosis are promising building blocks for tumor vaccines due to their abundant content of tumor antigens and immune-activating factors. The proteomics and genetic sequencing confirmed that pyosomes contain a much larger amount of inflammatory proteins, including immune-stimulating factors (e.g., DAMPs), and inflammasome-related microRNAs, compared to tumor exosomes that serve as a head-to-head comparison control in this study.

[0087] In multiple mouse models, the results demonstrated the potential of pyosome vaccines in generating local T cell responses against tumor recurrence after surgery and eliciting strong systemic immune responses against tumor metastasis. To further evaluate the antigen-specific immune response, in this study, both an artificial antigen OVA and a neoantigen Adpgk were implemented to investigate the antigen-specific DC and T cell immunity. Notably, there was a 10.7-fold increase in OVA-specific T cells (Pyo-R@Gel vs. blank Gel) and a 12.2-fold increase in Adpgk-specific T cells (Pyo-R@Gel vs. blank Gel). Finally, to substantiate the potential of pyosomes as a personalized vaccine, the pyosomes from the isolated patients' tumor samples were prepared and evaluated for therapeutic efficacy against a PDX TNBC-bearing humanized mouse model. The pyosomes displayed much better treatment outcomes compared to exosome vaccines. These results highlight both the translation potential of pyosome vaccines against human tumors and their customizability against individual patients.

[0088] The use of the terms "a" and "an" and "the" and similar referents (especially in the context of the following claims) are to be construed to cover both the singular and the plural, unless otherwise indicated herein or clearly contradicted by context. The terms first, second etc. as used herein are not meant to denote any particular ordering, but simply for convenience to denote a plurality of, for example, layers. The terms "comprising", "having", "including", and "containing" are to be construed as open-ended terms (i.e., meaning "including, but not limited to") unless otherwise noted. Recitation of ranges of values are

merely intended to serve as a shorthand method of referring individually to each separate value falling within the range, unless otherwise indicated herein, and each separate value is incorporated into the specification as if it were individually recited herein. The endpoints of all ranges are included within the range and independently combinable. All methods described herein can be performed in a suitable order unless otherwise indicated herein or otherwise clearly contradicted by context. The use of any and all examples, or exemplary language (e.g., "such as"), is intended merely to better illustrate the invention and does not pose a limitation on the scope of the invention unless otherwise claimed. No language in the specification should be construed as indicating any non-claimed element as essential to the practice of the invention as used herein.

[0089] While the invention has been described with reference to an exemplary embodiment, it will be understood by those skilled in the art that various changes may be made and equivalents may be substituted for elements thereof without departing from the scope of the invention. In addition, many modifications may be made to adapt a particular situation or material to the teachings of the invention without departing from the essential scope thereof. Therefore, it is intended that the invention not be limited to the particular embodiment disclosed as the best mode contemplated for carrying out this invention, but that the invention will include all embodiments falling within the scope of the appended claims. Any combination of the above-described elements in all possible variations thereof is encompassed by the invention unless otherwise indicated herein or otherwise clearly contradicted by context.

Claims

1. A method of preparing isolated pyosomes, comprising

providing an *ex-vivo* tumor cell,

treating the tumor cell with a pyroptosis-inducing agent under conditions for the tumor cell to undergo pyroptosis and produce pyosomes, and

isolating the pyosomes from the treated tumor cells.

2. The method of claim 1, further comprising, prior to isolating the pyosomes, imaging the treated tumor cells to verify a pyroptosis morphology, to verify pyosomes protruding from or excreted from the tumor cell surface, or a combination thereof.

3. The method of claim 2, wherein imaging comprises scanning electron microscopy, confocal microscopy, or a combination thereof.

4. The method of claim 1, wherein the pyosomes are isolated from a tumor from a patient with cancer.

5. The method of claim 4, wherein the patient has triple negative breast cancer, malignant melanoma, lung cancer, ovarian cancer, colon cancer, prostate cancer, bladder cancer, a sarcoma, a lymphoma which produces solid tumors, or liver cancer.

6. The method of claim 1, wherein the pyroptosis-inducing agent comprises lipopolysaccharide and nigericin, gramicidin, a bacterial toxin, a reactive oxygen species (ROS), lipopolysaccharide and adenosinetriphosphate (ATP), polyphyllin VI, 6,7-dichloro-2-methylsulfonyl-3-N-tert-butylaminoquinoxaline (DMB), photodynamic therapy (PDT), or a combination thereof.

7. The method of claim 1, wherein isolating the pyosomes from the treated tumor cells comprises gradient centrifugation, size-based isolation, microfluidic isolation, a membrane affinity spin column, or a combination thereof.

8. The method of claim 1, wherein the diameters of the isolated pyosomes are distributed between 100 nm and 1000 nm.

9. The method of claim 1, wherein the isolated pyosomes have a zeta potential of about -8 mv.

10. The method of claim 1, wherein the isolated pyosomes comprise more than 2000 different types of proteins as determined by proteomic analysis, and exhibit higher levels of high mobility group box 1 protein (HMGB1), heat shock protein 70 (HSP70), and calreticulin compared to tumor exosomes.

11. The method of claim 1, wherein the isolated pyosomes express elevated levels of microRNAs expressed in AMPK and PI3K-Akt signaling pathways compared to tumor exosomes.

12. The method of claim 1, further comprising preparing an immunostimulant composition by loading an immunostimulant into the isolated pyosomes.

13. The method of claim 12, wherein the immunostimulant comprises resiquimod, imiquimod, gardiquimod, SEQ ID NO: 2, agatolimod, diprovocim, telratolimod, motolimod, vesatolimod, polyinosinic-polycytidylic acid sodium, paclitaxel, adriamycin, levamisole, a small molecule immune checkpoint inhibitor, or a combination thereof.

14. The product of the process of any of claims 1-13.

15. A pharmaceutical composition comprising the immunostimulant composition of claim 12 or 13 and a pharmaceutically acceptable carrier.

16. An implantable pharmaceutical composition comprising the immunostimulant composition of claim 12 or 13 suspended in a polymeric carrier.

17. The implantable composition of claim 16, wherein the polymeric carrier is a hydrogel.

18. A method of treating a patient in need of treatment for a solid tumor, comprising administering to the patient the implantable pharmaceutical composition of claim 16 or 17.

19. The method of claim 18, wherein the patient is in need of treatment for post-surgical tumor recurrence of the solid tumor.

20. The method of claim 18, wherein the pyosomes were isolated from tumor cells removed from the patient.

21. The method of claim 18, wherein administering comprises injecting or implanting the pharmaceutical composition at the surgical site.

22. The method of claim 18, wherein the patient has triple negative breast cancer, malignant melanoma, lung cancer, ovarian cancer, colon cancer, bladder cancer, a sarcoma, a lymphoma which produces solid tumors, liver cancer, or prostate cancer.

23. The method of claim 18, further comprising administering a chemotherapeutic agent, a radiotherapeutic agent, or a combination thereof.

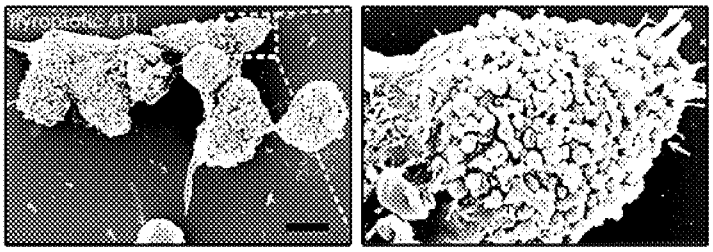

Fig. 1a

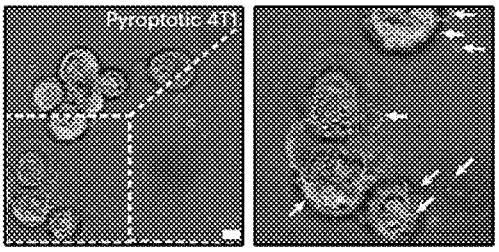

Fig. 1b

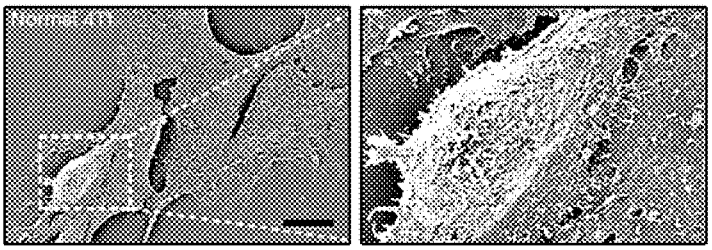

Fig. 1c

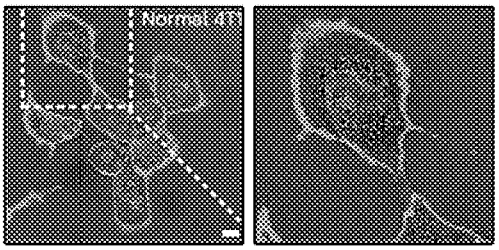

Fig. 1d

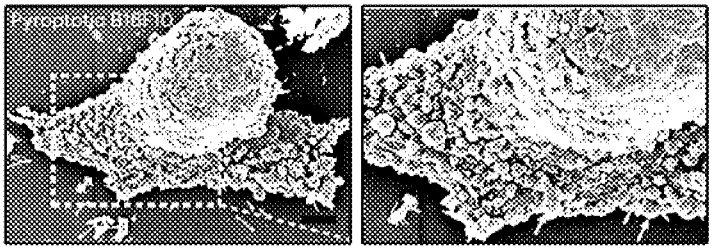

Fig. 1e

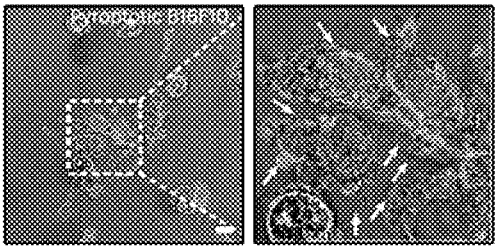

Fig. 1f

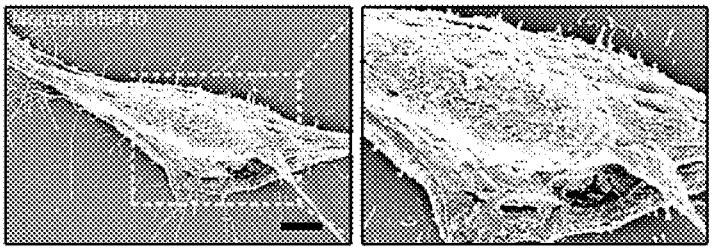

Fig. 1g

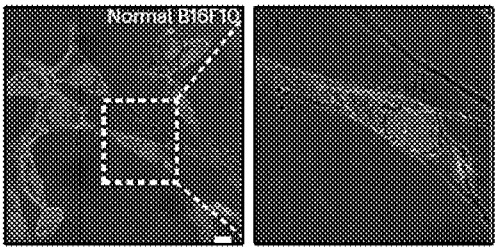

Fig. 1h

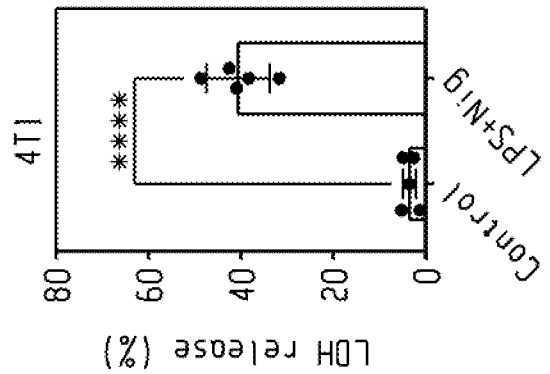

Fig. 2b

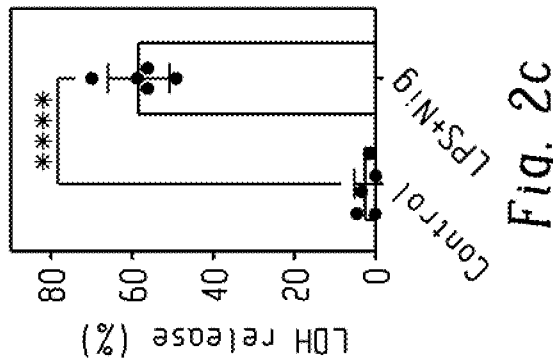

Fig. 2c

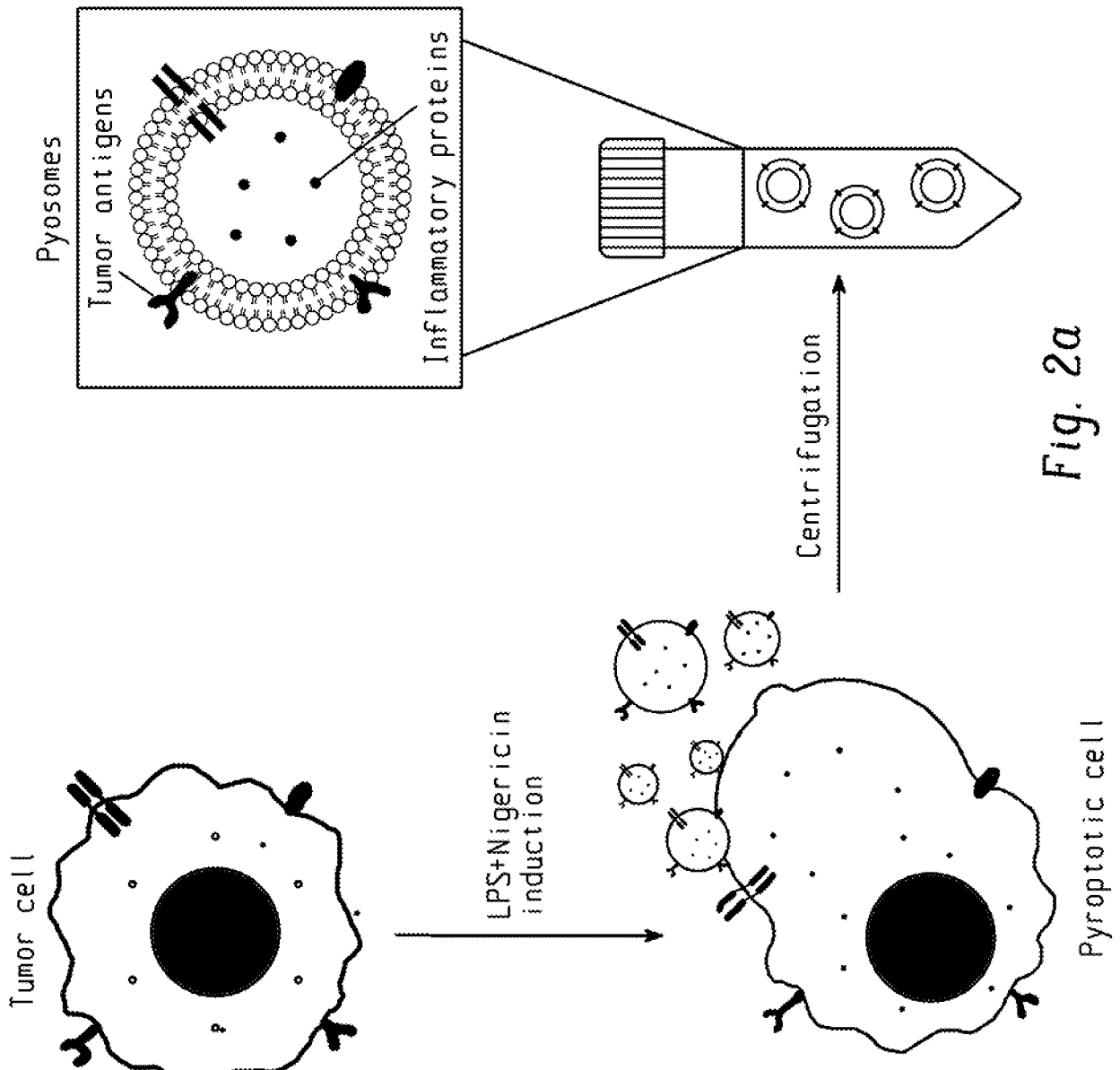

Fig. 2a

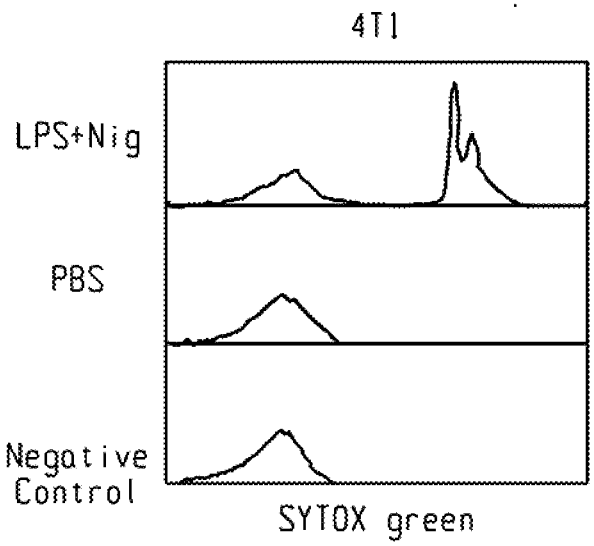

Fig. 2d

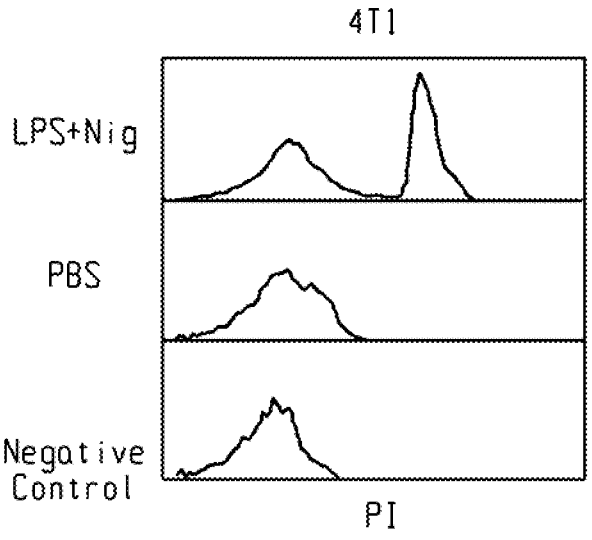

Fig. 2e

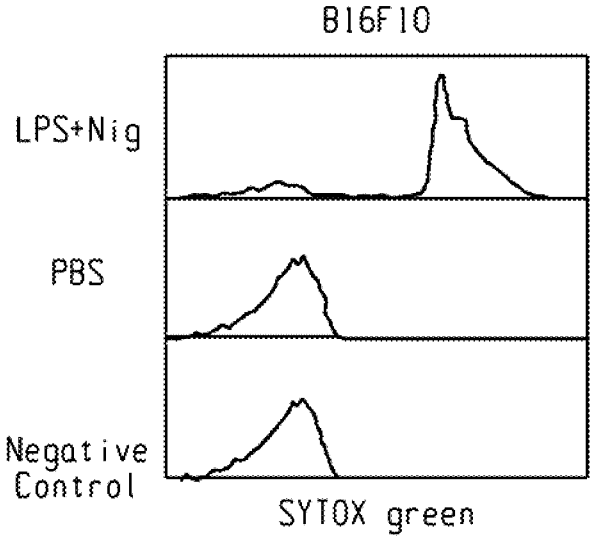

Fig. 2f

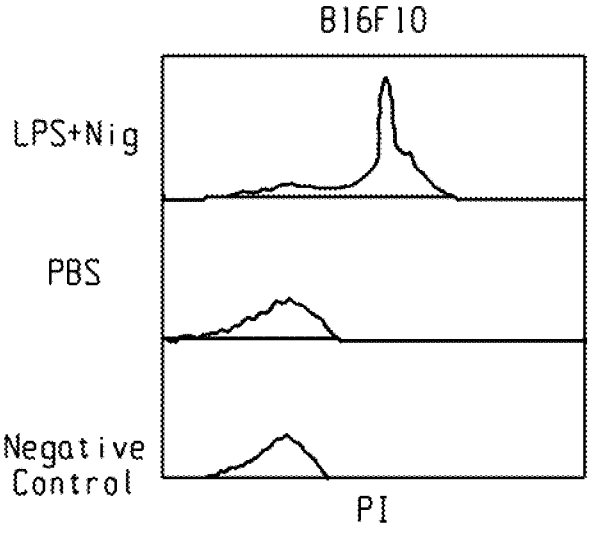

Fig. 2g

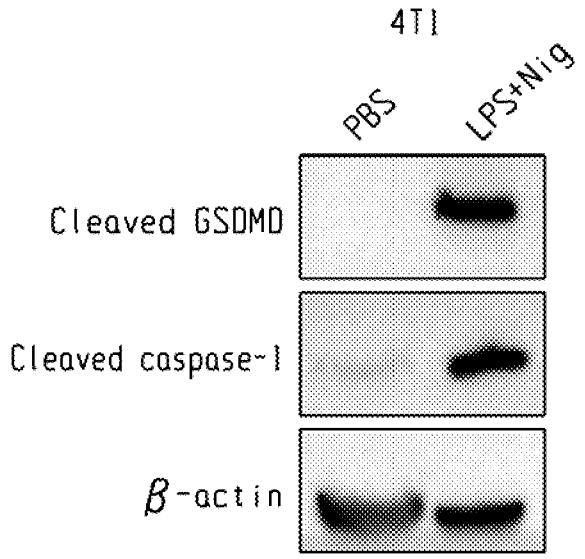

Fig. 2h

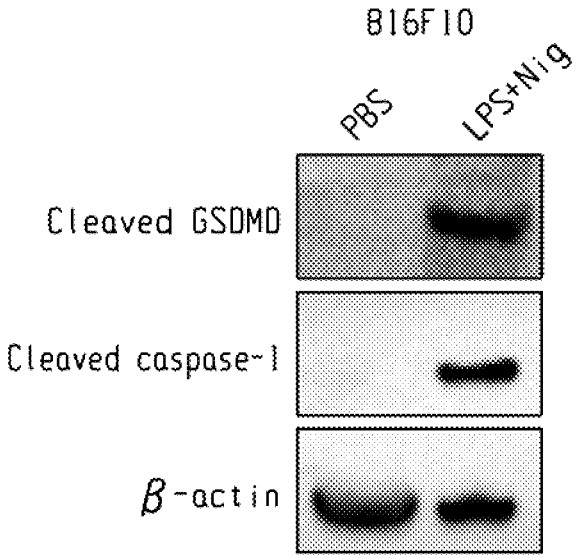

Fig. 2i

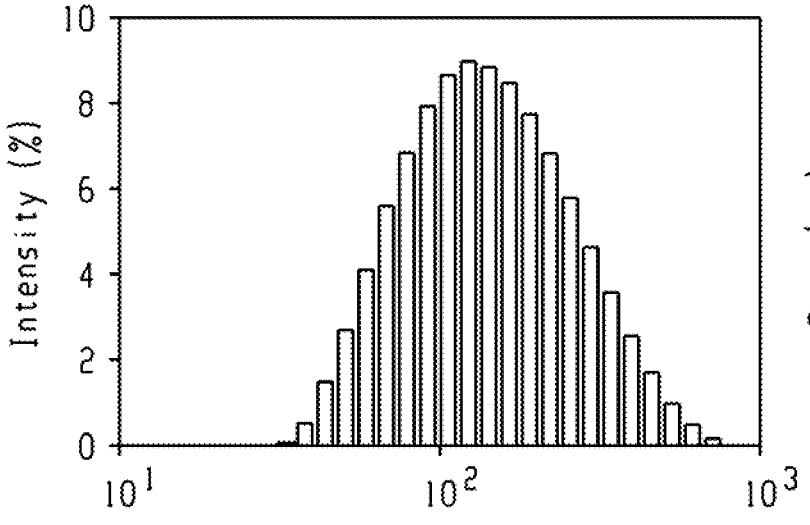

Fig. 2j

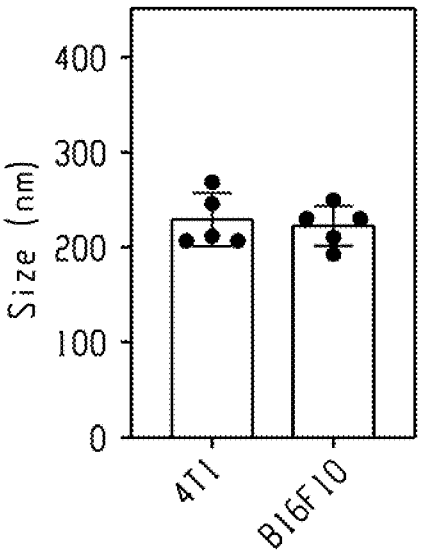

Fig. 2k

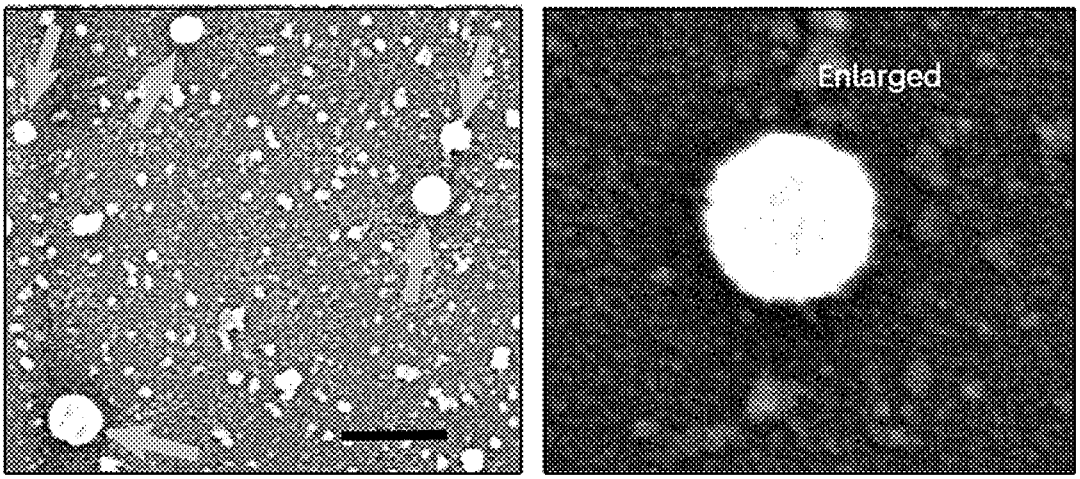

Fig. 2l

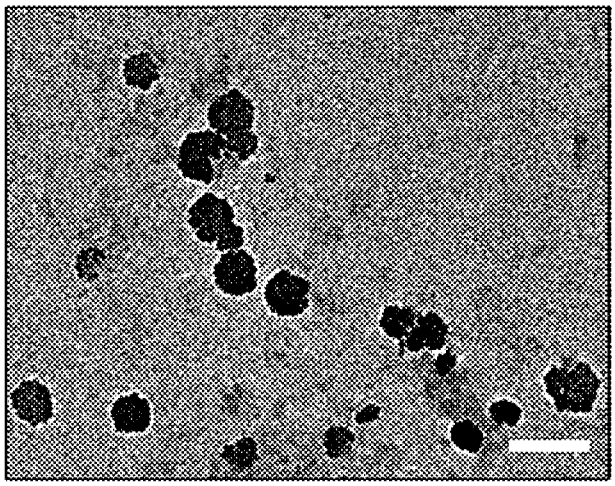

Fig. 2m

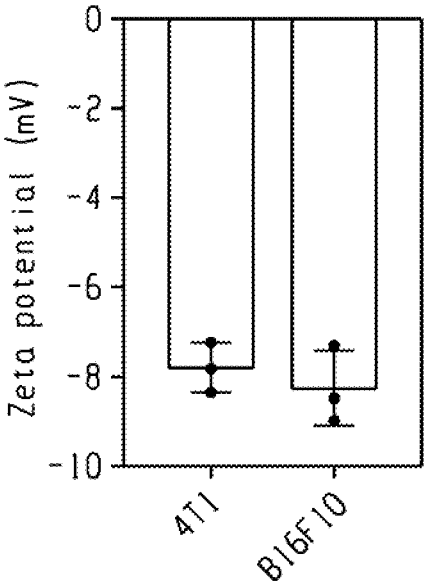

Fig. 2n

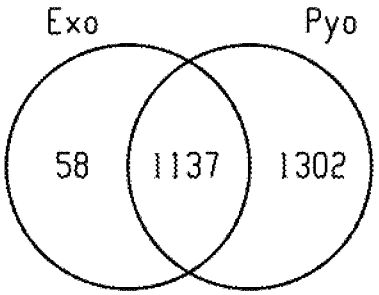

Fig. 3a

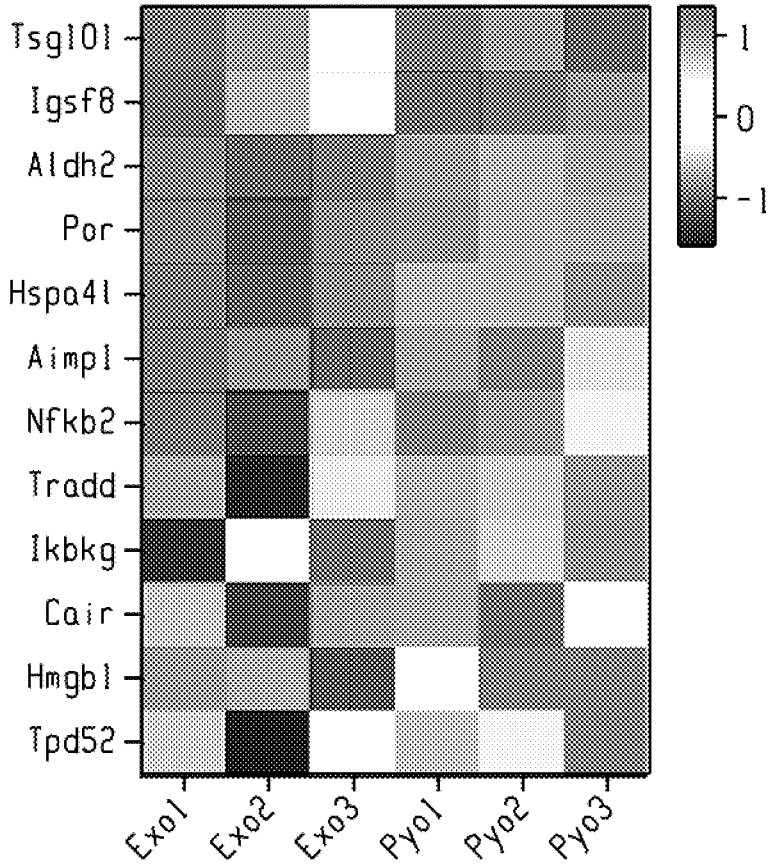

Fig. 3c

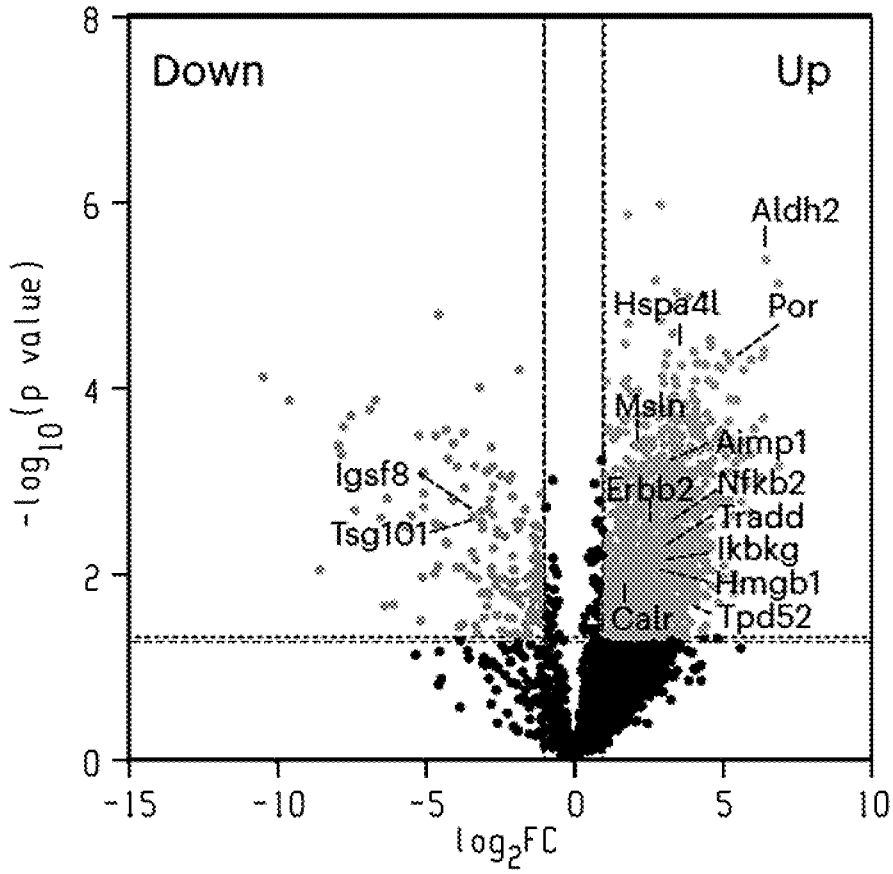

Fig. 3b

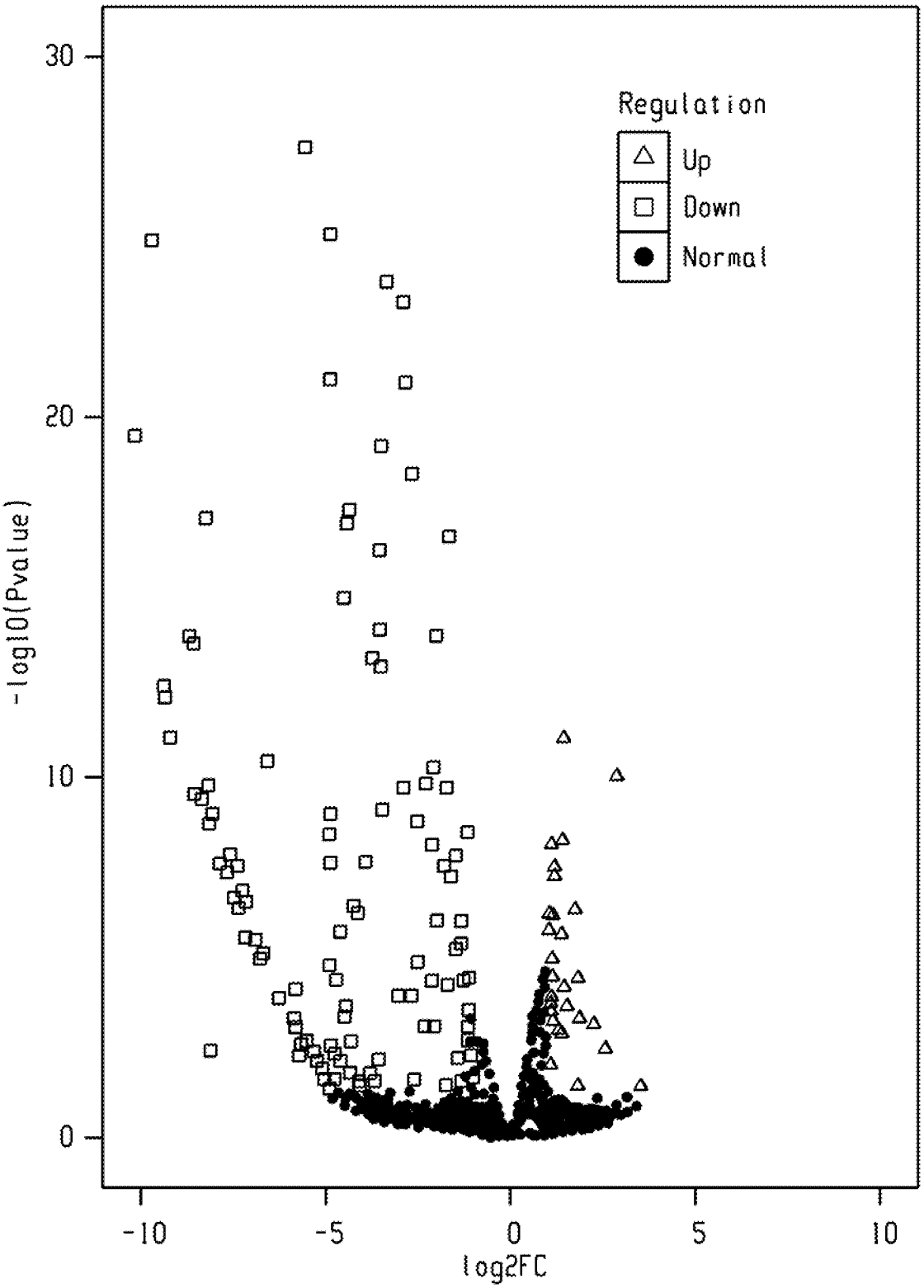
Regulation
Up
Down
Normal
30
20
10
0
-log10(Pvalue)
-10
-5
0
5
10
log2FC

Fig. 3d

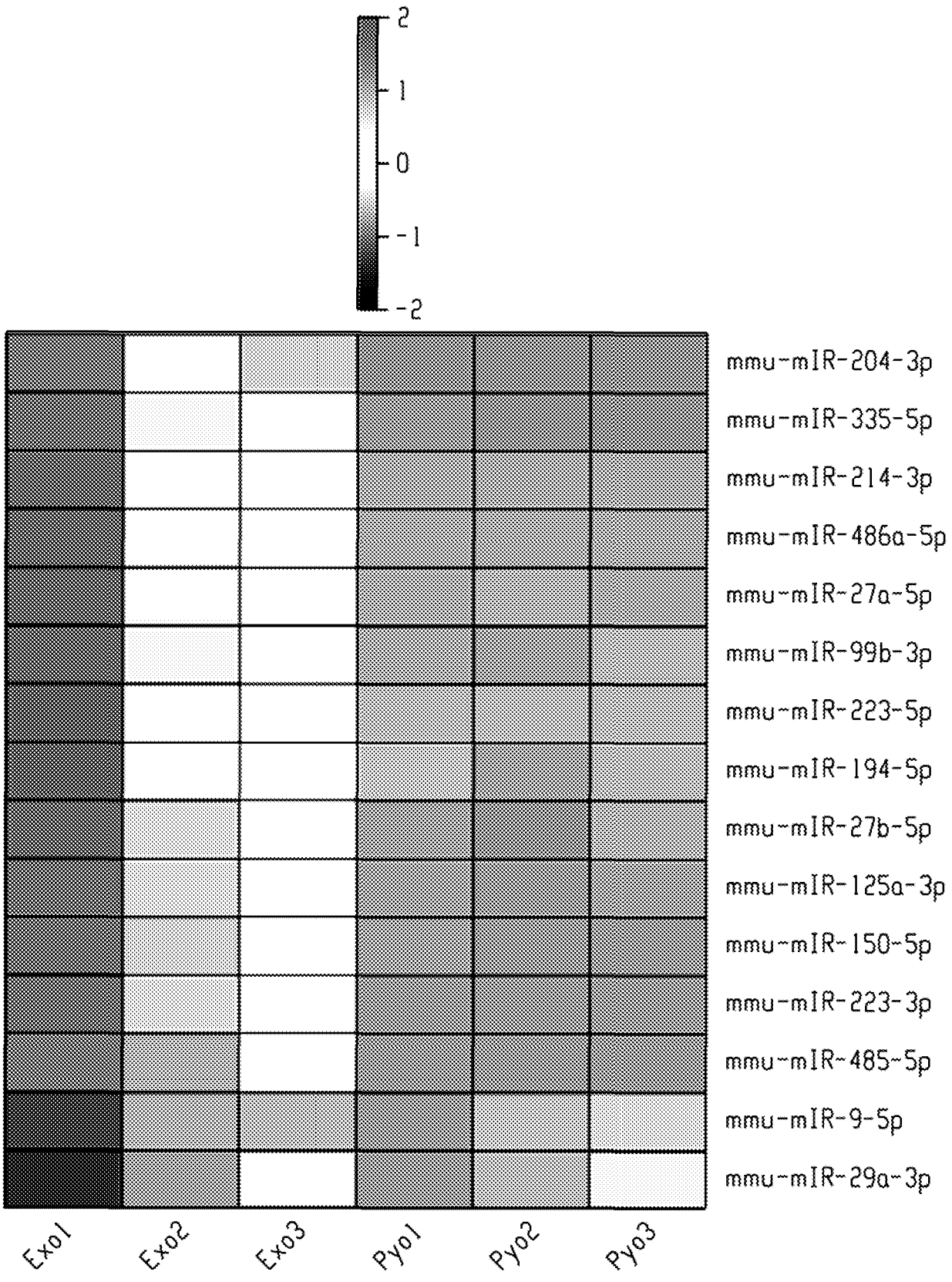
2
1
0
-1
-2
mmu-miR-204-3p
mmu-miR-335-5p
mmu-miR-214-3p
mmu-miR-486a-5p
mmu-miR-27a-5p
mmu-miR-99b-3p
mmu-miR-223-5p
mmu-miR-194-5p
mmu-miR-27b-5p
mmu-miR-125a-3p
mmu-miR-150-5p
mmu-miR-223-3p
mmu-miR-485-5p
mmu-miR-9-5p
mmu-miR-29a-3p
Exo1
Exo2
Exo3
Pyo1
Pyo2
Pyo3

Fig. 3e

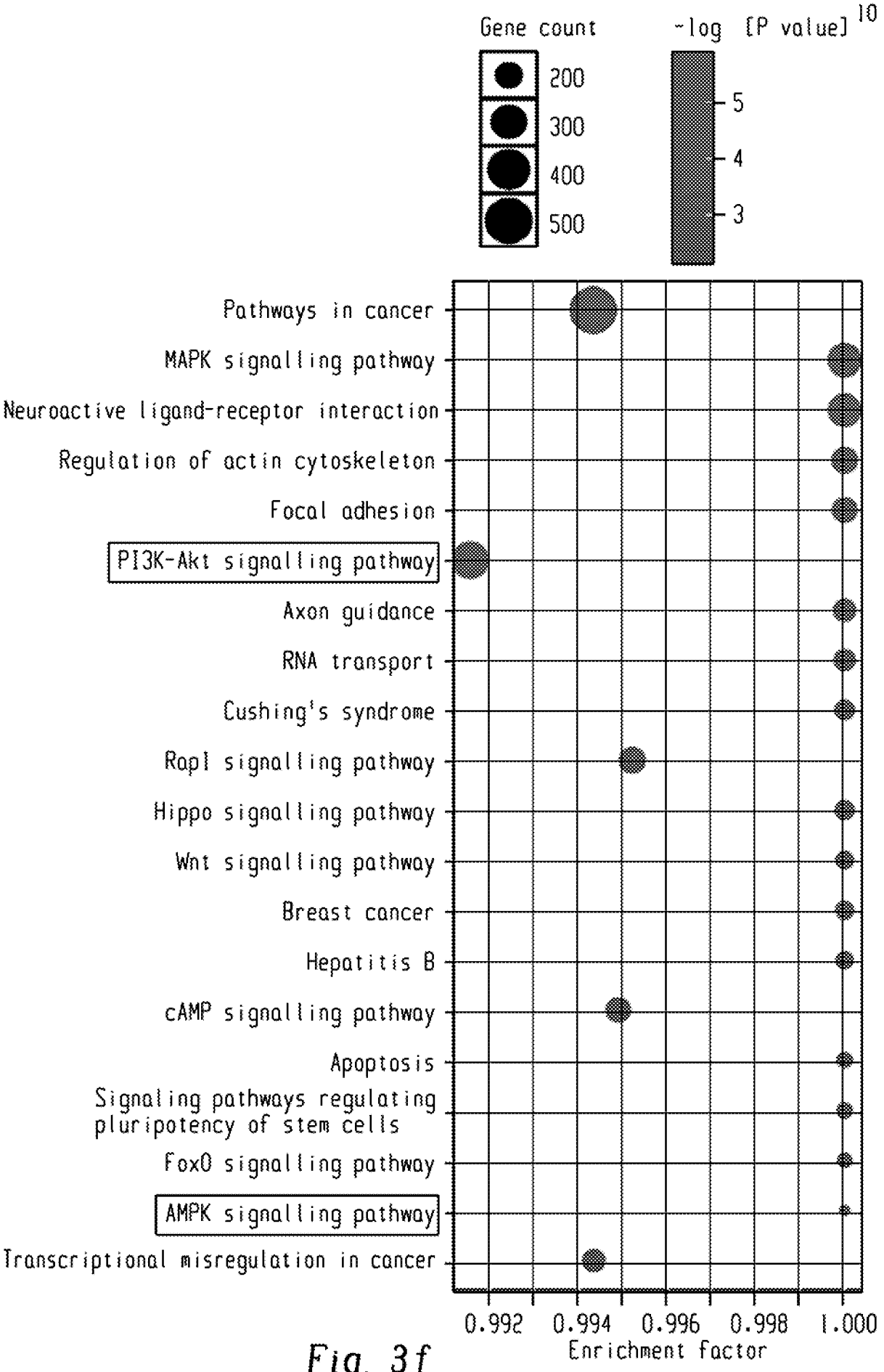
Gene count
200
300
400
500
-log [P value] 10
5
4
3
Pathways in cancer
MAPK signalling pathway
Neuroactive ligand-receptor interaction
Regulation of actin cytoskeleton
Focal adhesion
PI3K-Akt signalling pathway
Axon guidance
RNA transport
Cushing's syndrome
Rapl signalling pathway
Hippo signalling pathway
Wnt signalling pathway
Breast cancer
Hepatitis B
cAMP signalling pathway
Apoptosis
Signaling pathways regulating pluripotency of stem cells
FoxO signalling pathway
AMPK signalling pathway
Transcriptional misregulation in cancer
0.992
0.994
0.996
0.998
1.000
Enrichment factor

Fig. 3f

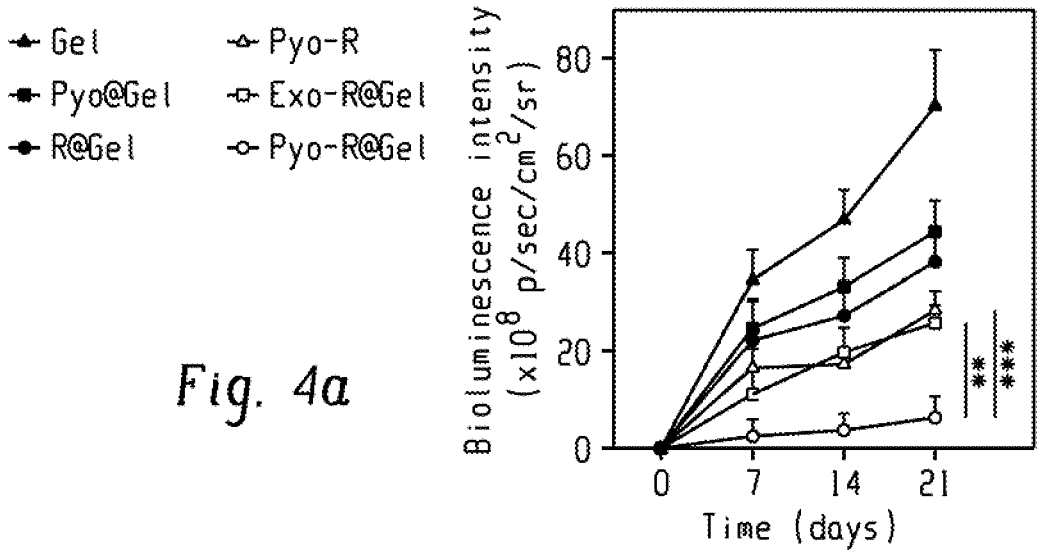

Fig. 4a

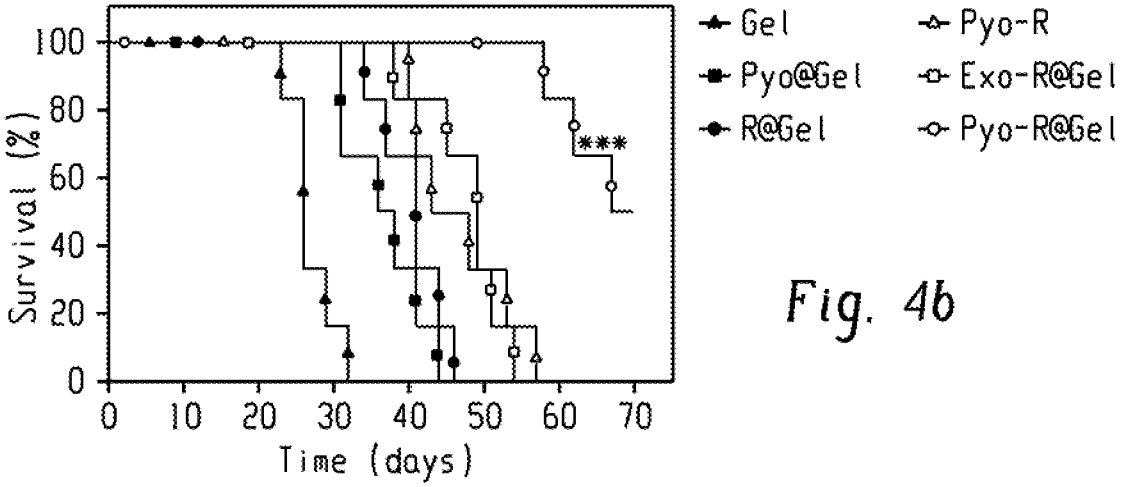

Fig. 4b

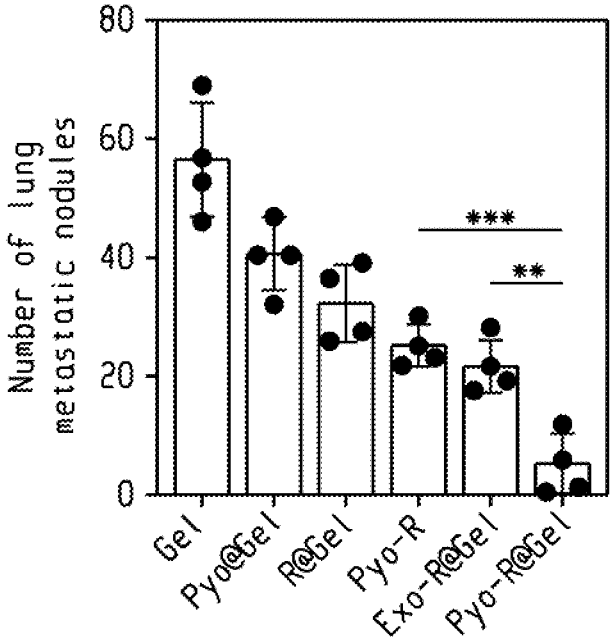

Fig. 4c

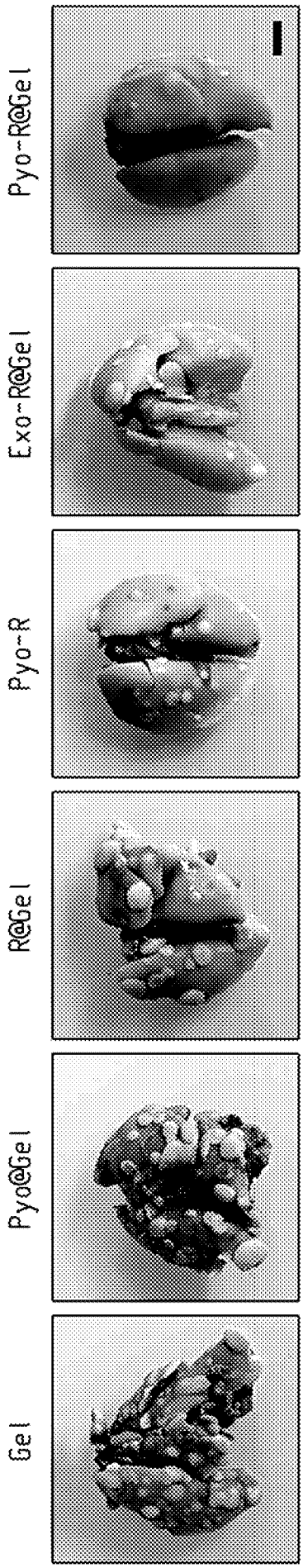
Gel
Pyo@Gel
R@Gel
Pyo-R
Exo-R@Gel
Pyo-R@Gel

Fig. 4d

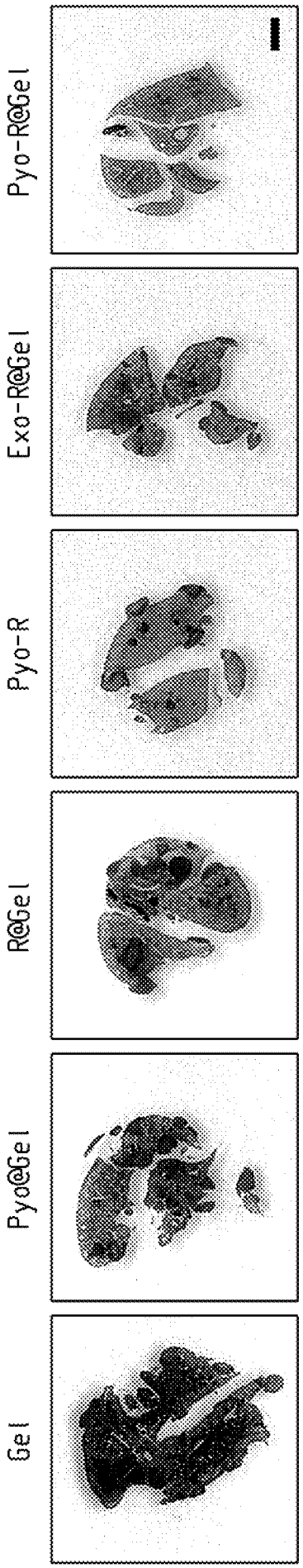
Gel
Pyo@Gel
R@Gel
Pyo-R
Exo-R@Gel
Pyo-R@Gel

Fig. 4e

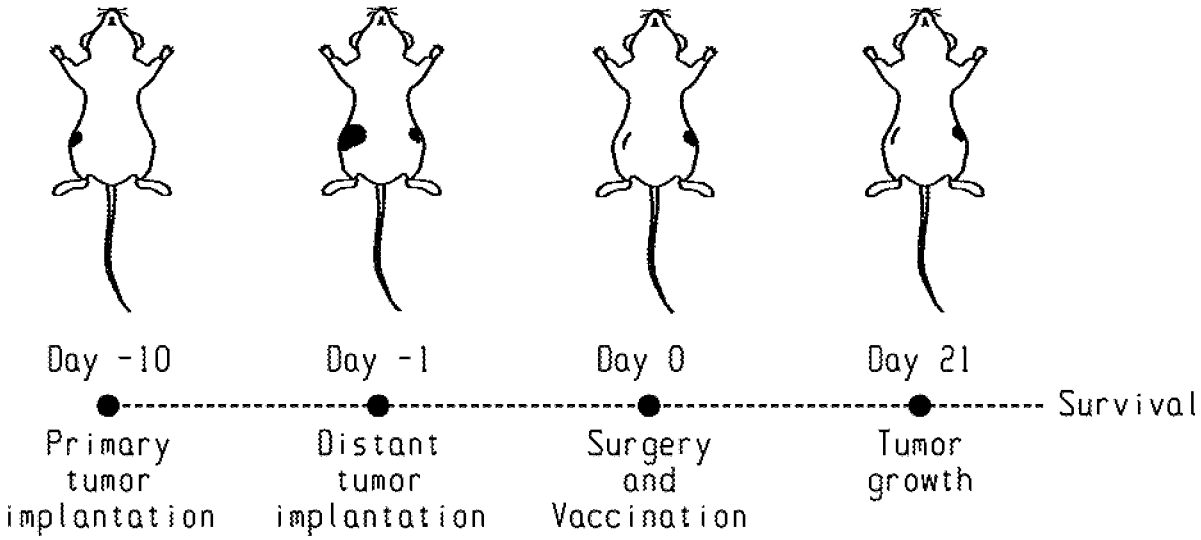

Fig. 4f

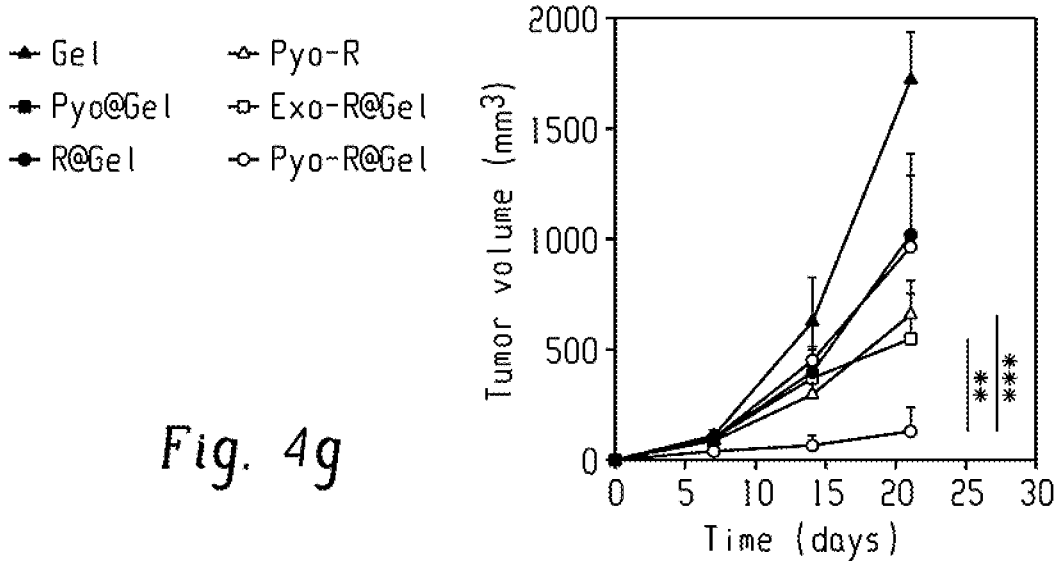

Fig. 4g

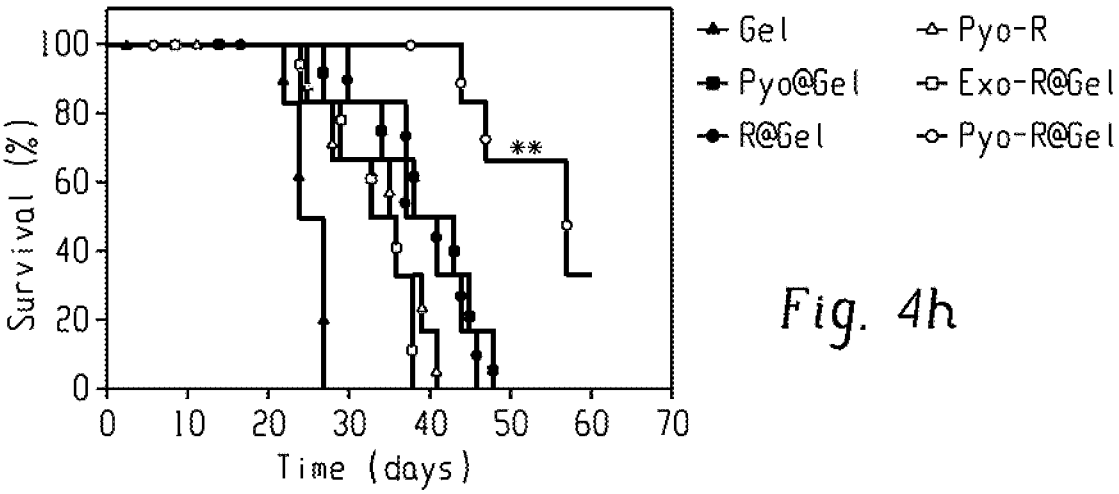

Fig. 4h

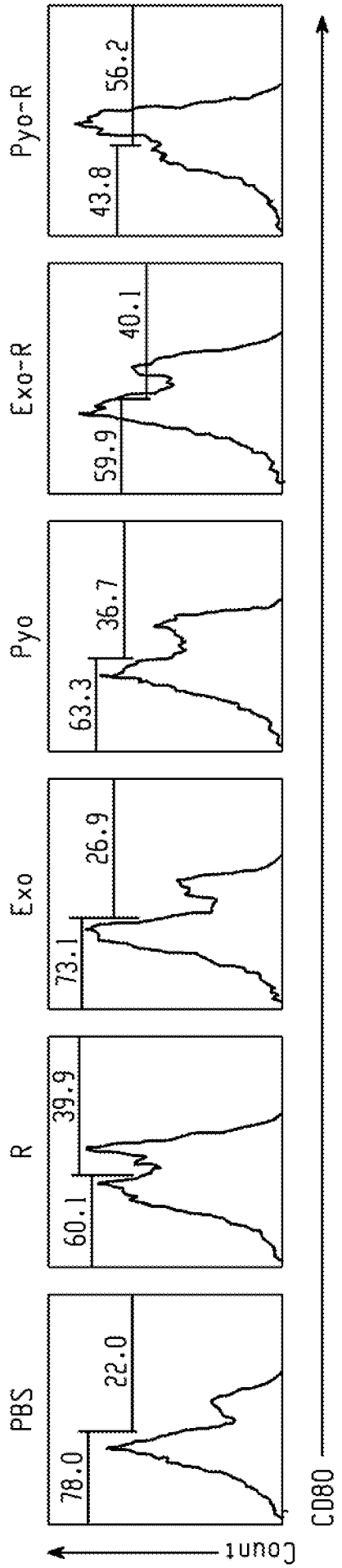
PBS
R
Exo
Pyo
Exo-R
Pyo-R
78.0
22.0
60.1
39.9
73.1
26.9
63.3
36.7
59.9
40.1
43.8
56.2
Count
CD80

Fig. 5a

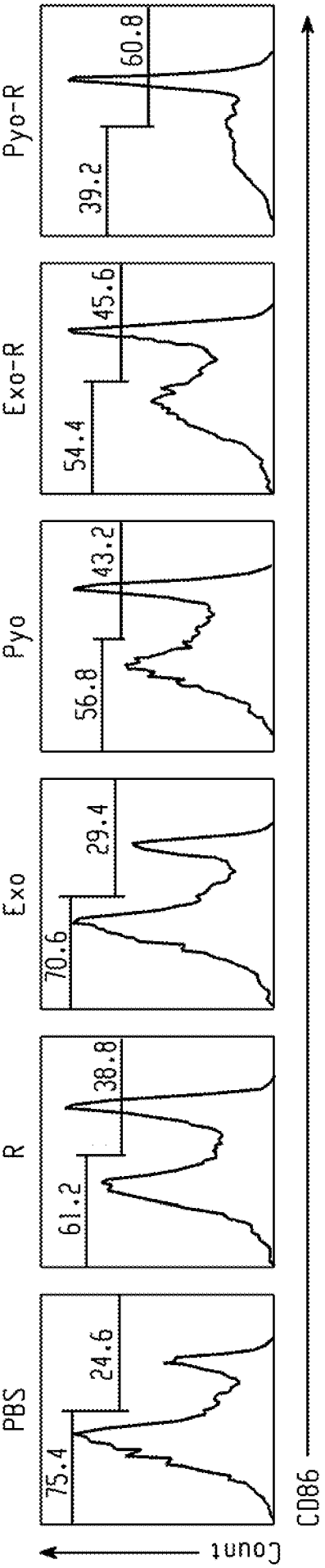
PBS
R
Exo
Pyo
Exo-R
Pyo-R
75.4
24.6
61.2
38.8
70.6
29.4
56.8
43.2
54.4
45.6
39.2
60.8
Count
CD86

Fig. 5b

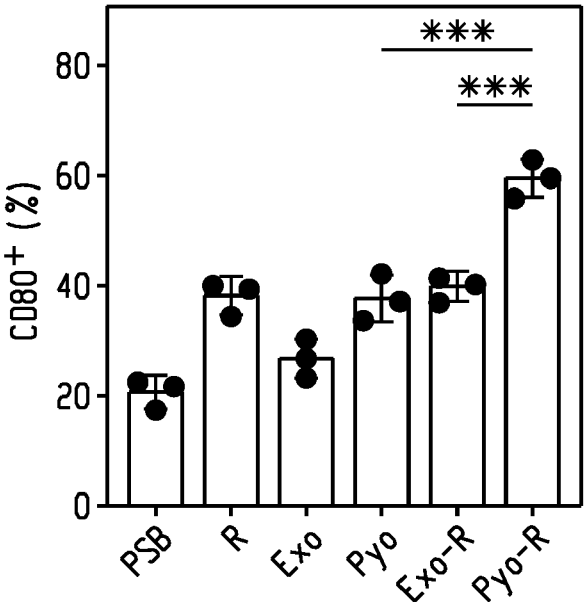

Fig. 5c

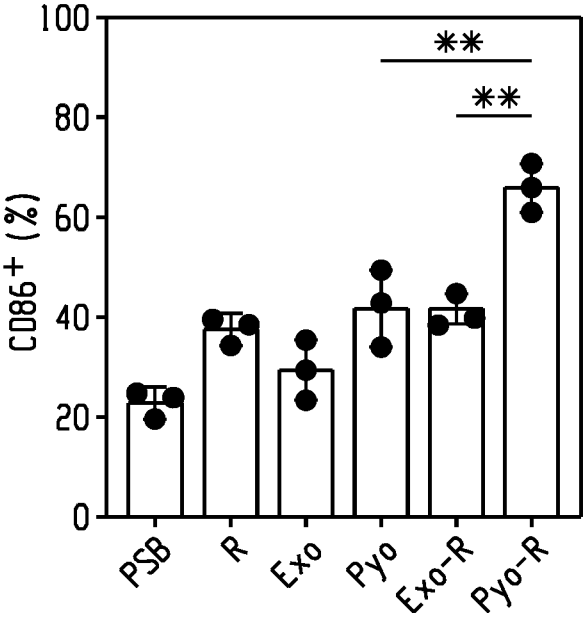

Fig. 5d

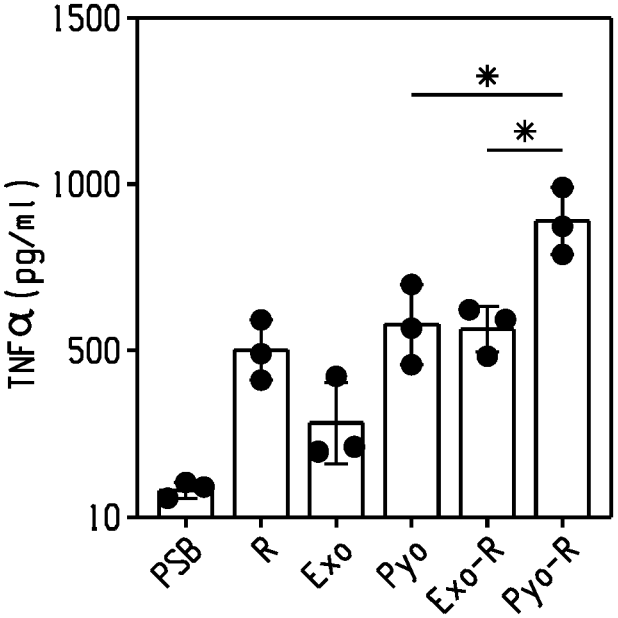

Fig. 5e

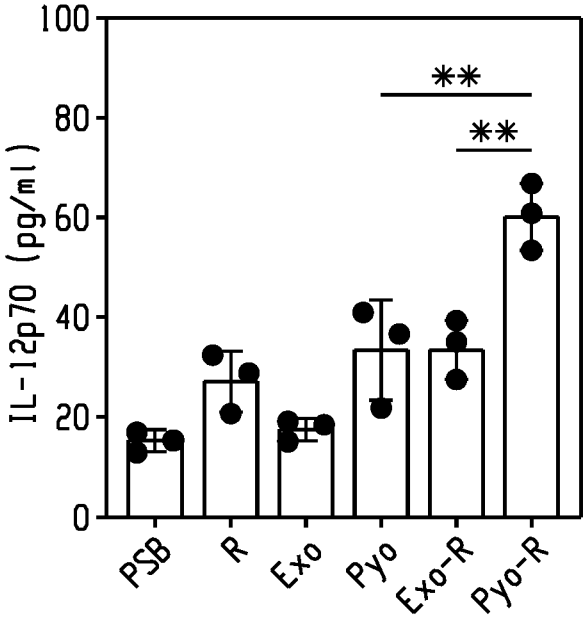

Fig. 5f

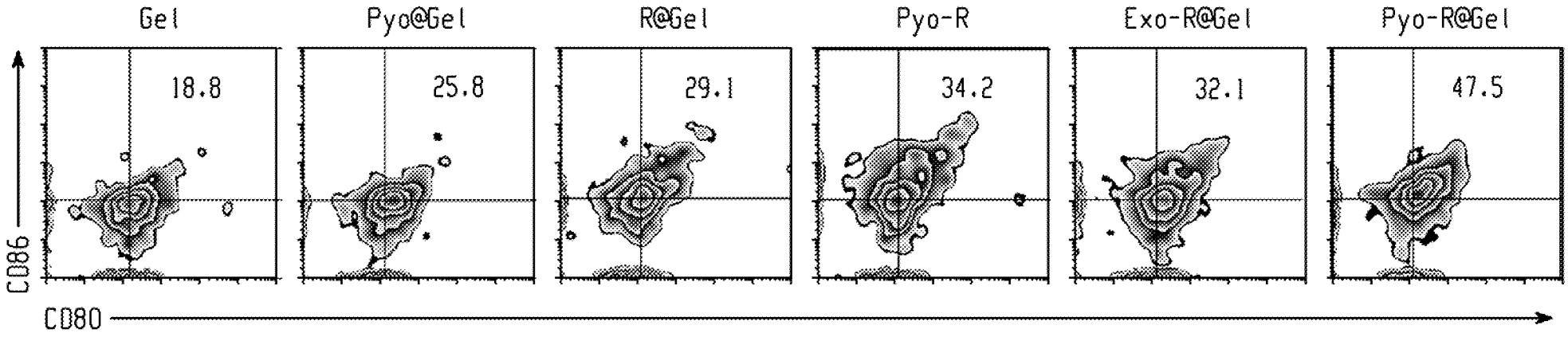
Gel
Pyo@Gel
R@Gel
Pyo-R
Exo-R@Gel
Pyo-R@Gel
18.8
25.8
29.1
34.2
32.1
47.5
CD86
CD80

Fig. 5g

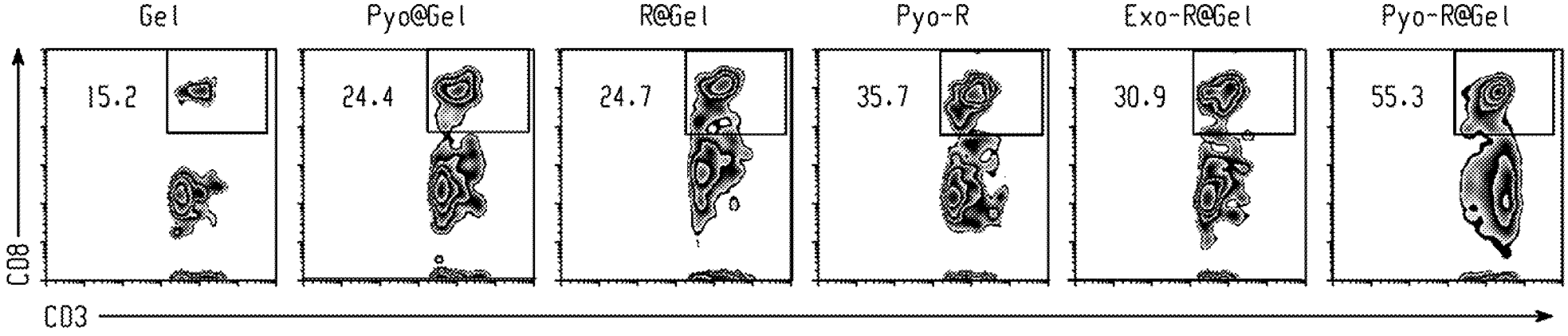
Gel
Pyo@Gel
R@Gel
Pyo-R
Exo-R@Gel
Pyo-R@Gel
15.2
24.4
24.7
35.7
30.9
55.3
CD8
CD3

Fig. 5h

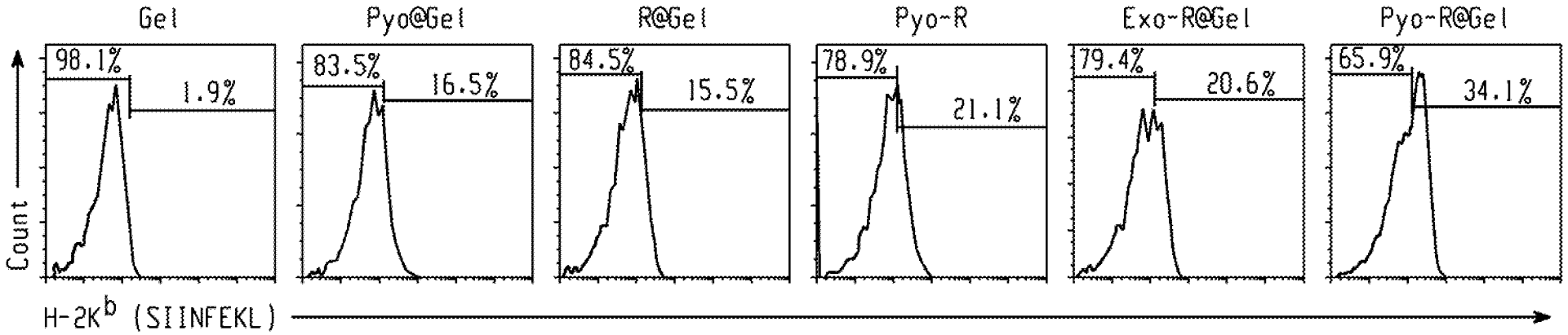
Gel
Pyo@Gel
R@Gel
Pyo-R
Exo-R@Gel
Pyo-R@Gel
98.1%
1.9%
83.5%
16.5%
84.5%
15.5%
78.9%
21.1%
79.4%
20.6%
65.9%
34.1%
Count
H-2K^{b} (SIINFEKL)

Fig. 6a

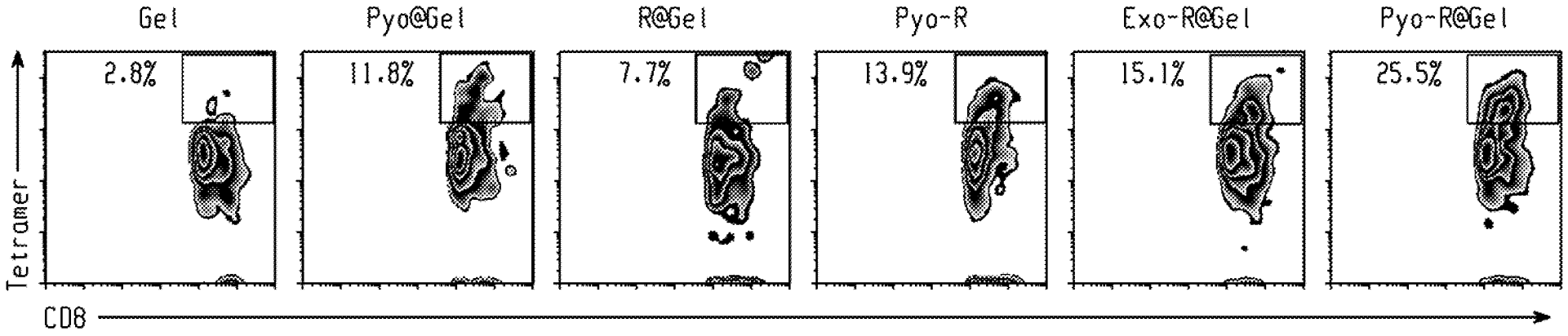
Gel
Pyo@Gel
R@Gel
Pyo-R
Exo-R@Gel
Pyo-R@Gel
2.8%
11.8%
7.7%
13.9%
15.1%
25.5%
Tetramer
CD8

Fig. 6b

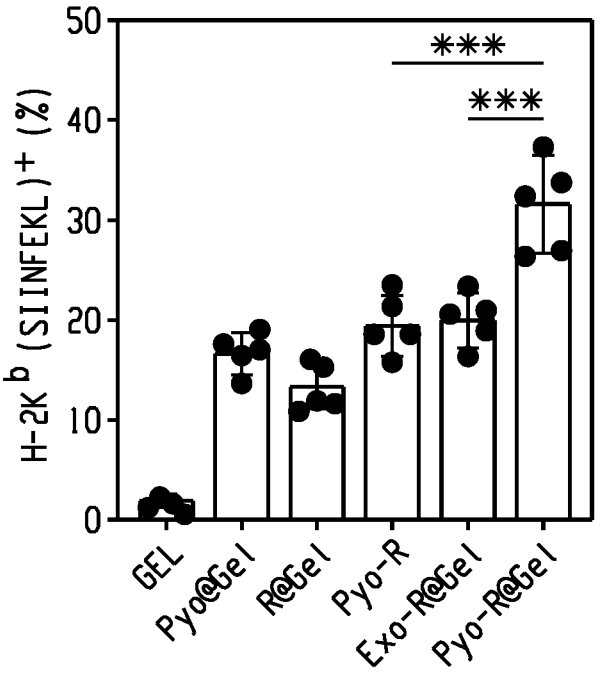

Fig. 6c

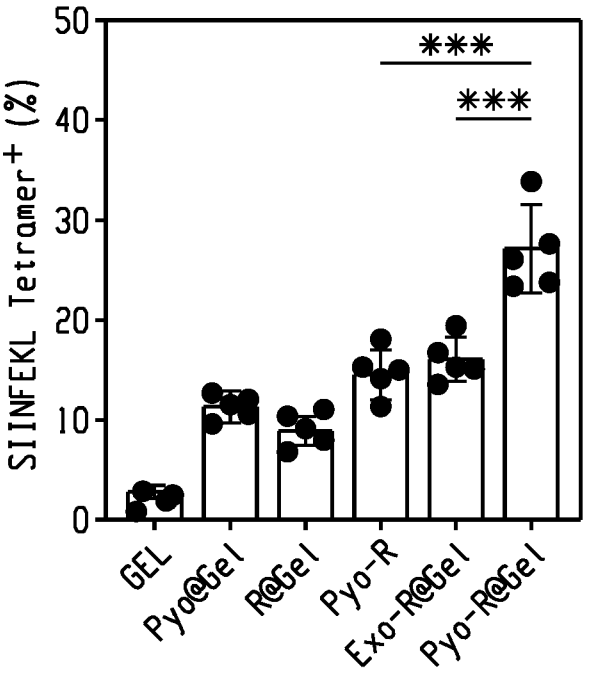

Fig. 6d

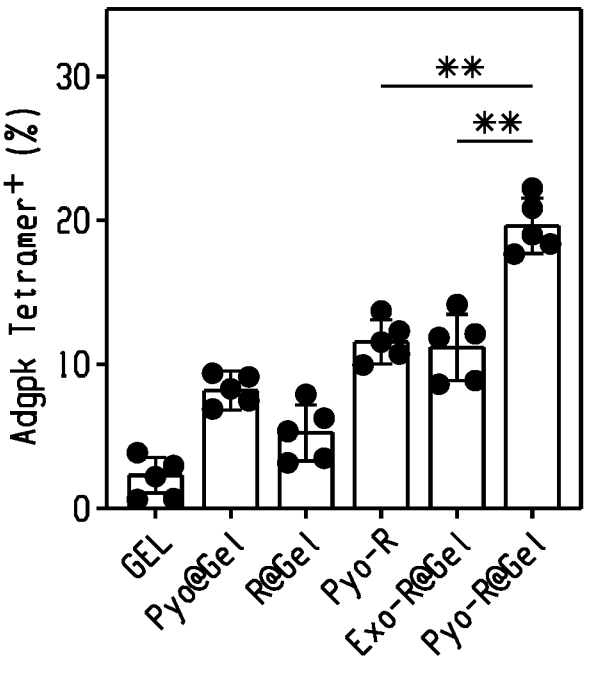

Fig. 6e

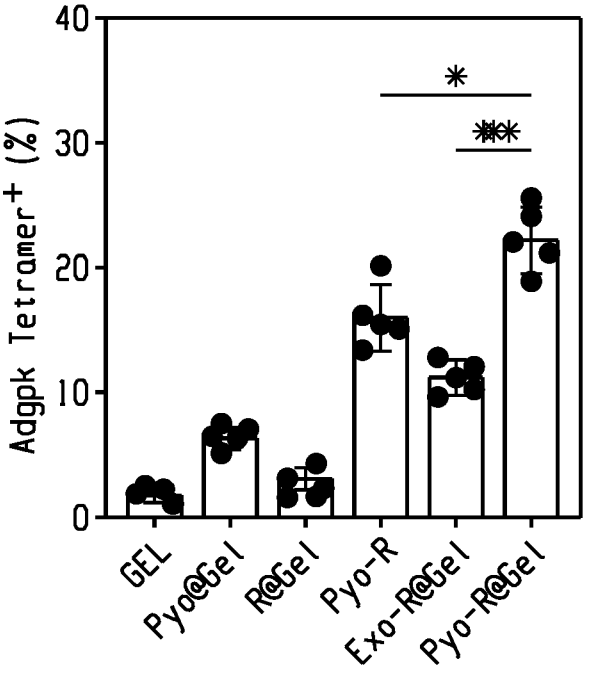

Fig. 6f

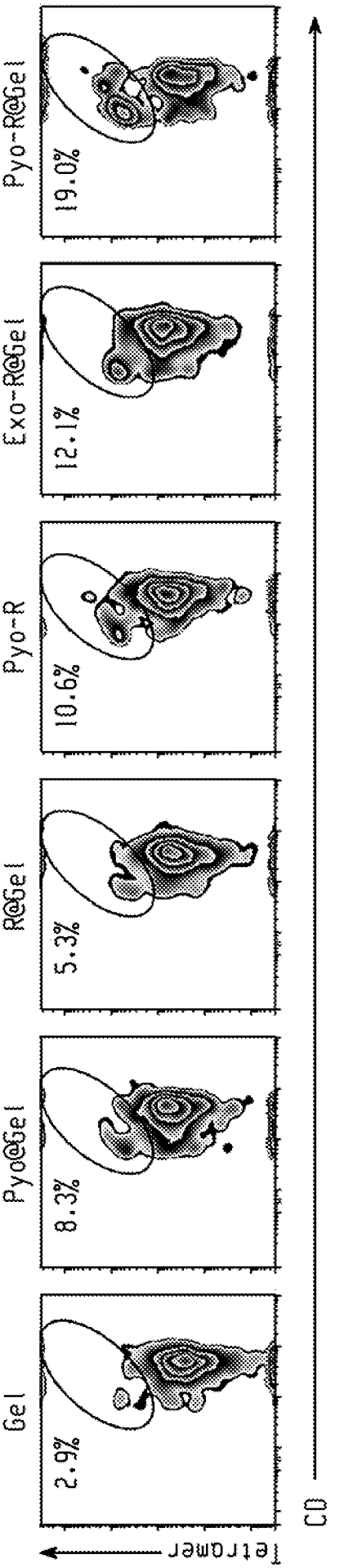
Gel
Pyo@Gel
R@Gel
Pyo-R
Exo-R@Gel
Pyo-R@Gel
2.9%
8.3%
5.3%
10.6%
12.1%
19.0%
Tetramer
CD

Fig. 6g

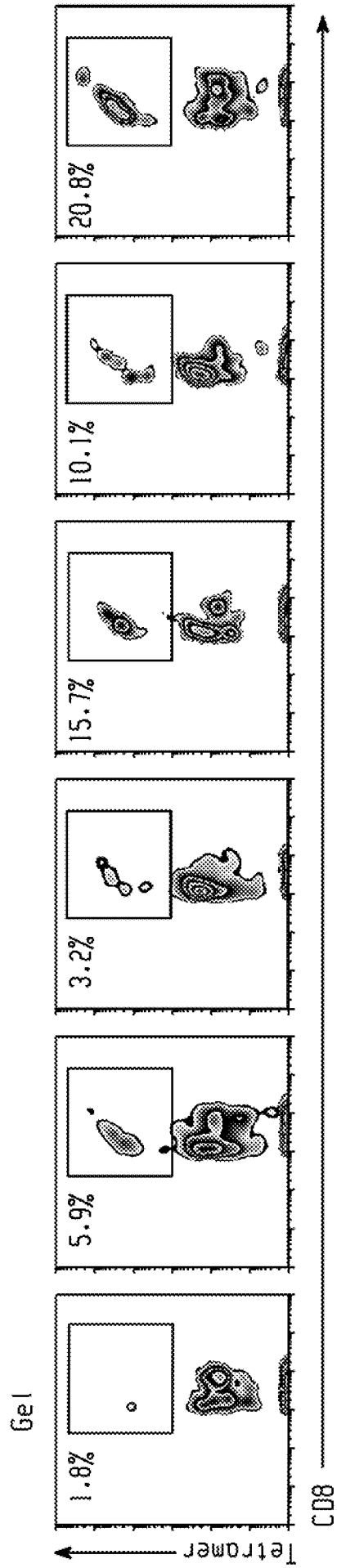
Gel
1.8%
5.9%
3.2%
15.7%
10.1%
20.8%
Tetramer
CD8

Fig. 6h

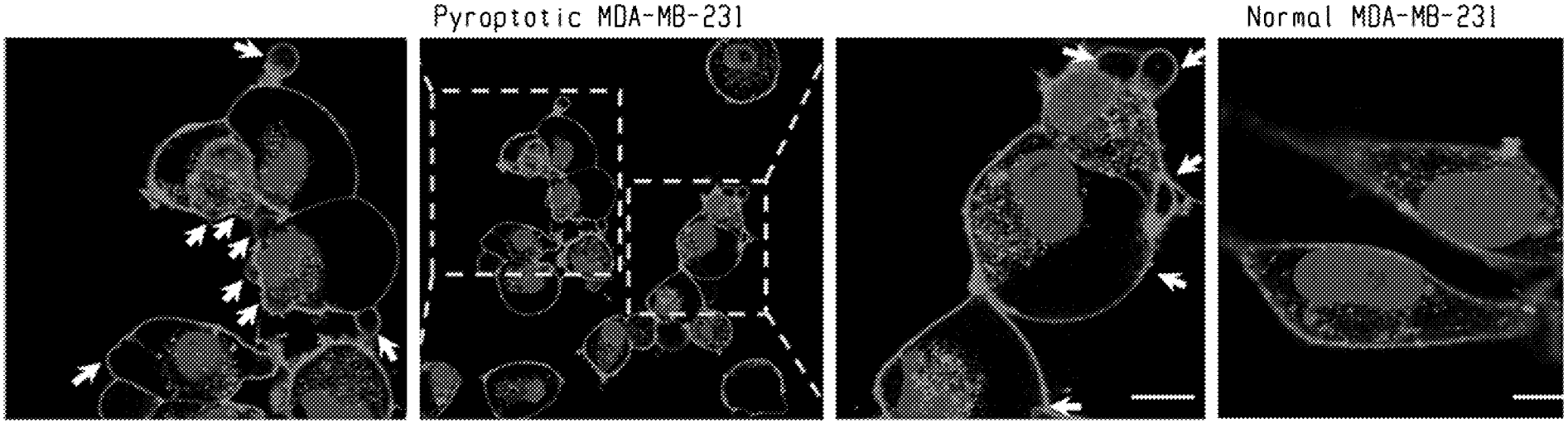

Fig. 7a

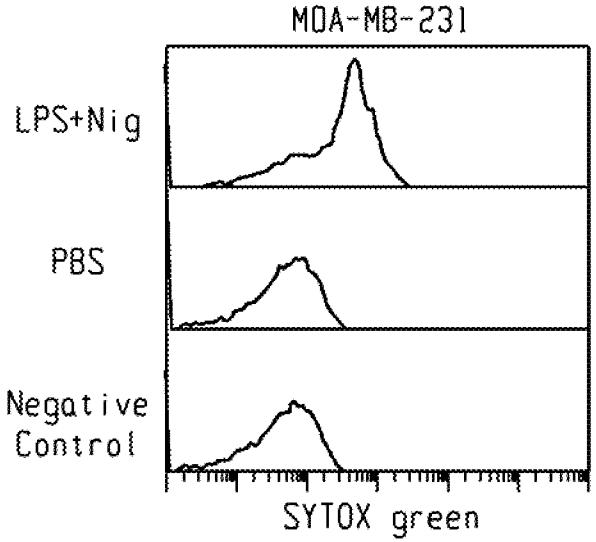

Fig. 7b

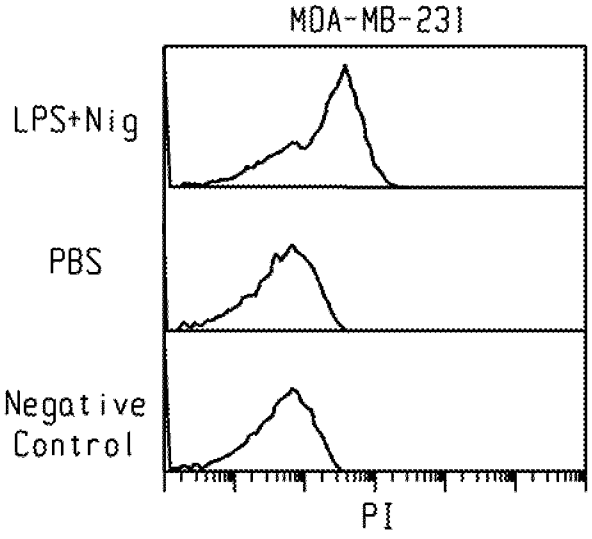

Fig. 7c

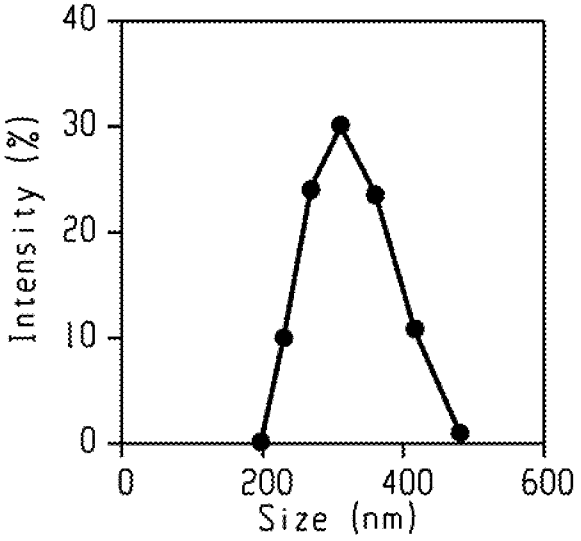

Fig. 7d

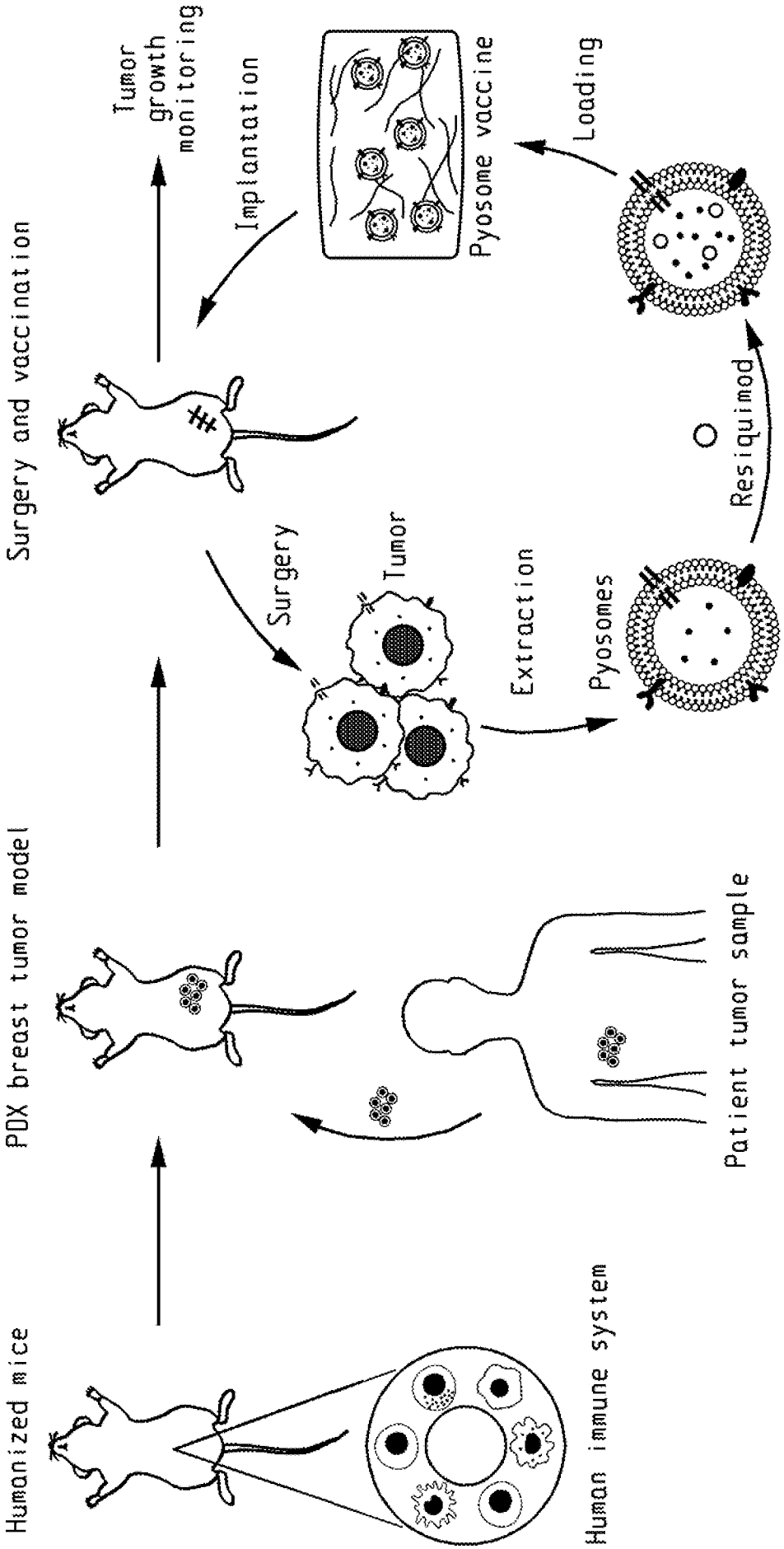
Humanized mice
Human immune system
PDX breast tumor model
Patient tumor sample
Surgery and vaccination
Surgery
Tumor
Extraction
Pyosomes
Resiquimod
Loading
Pyosome vaccine
Implantation
Tumor growth monitoring

Fig. 7e

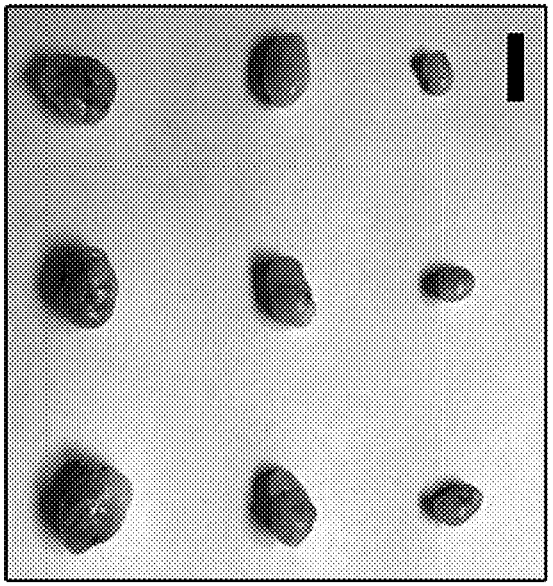

Fig. 7f

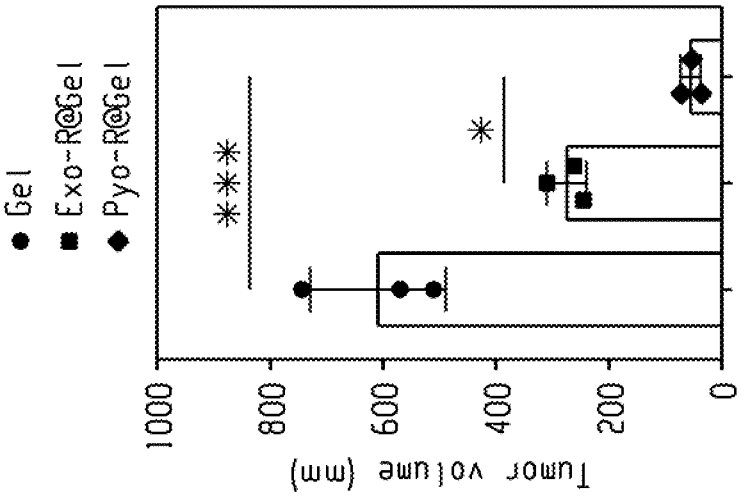

Fig. 7g

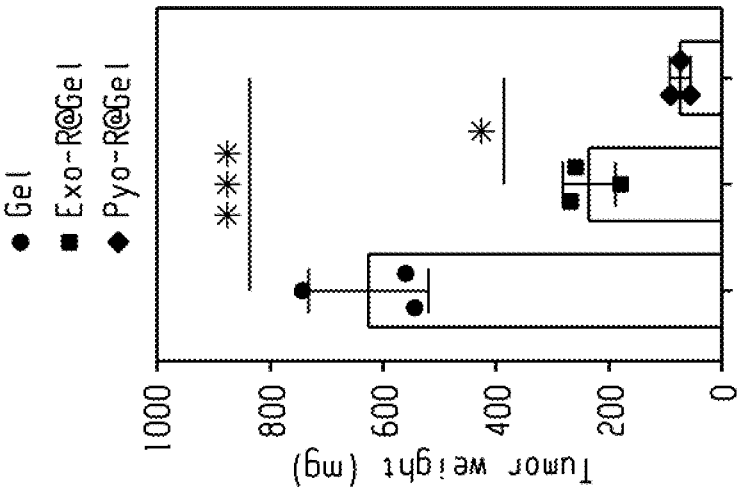

Fig. 7h

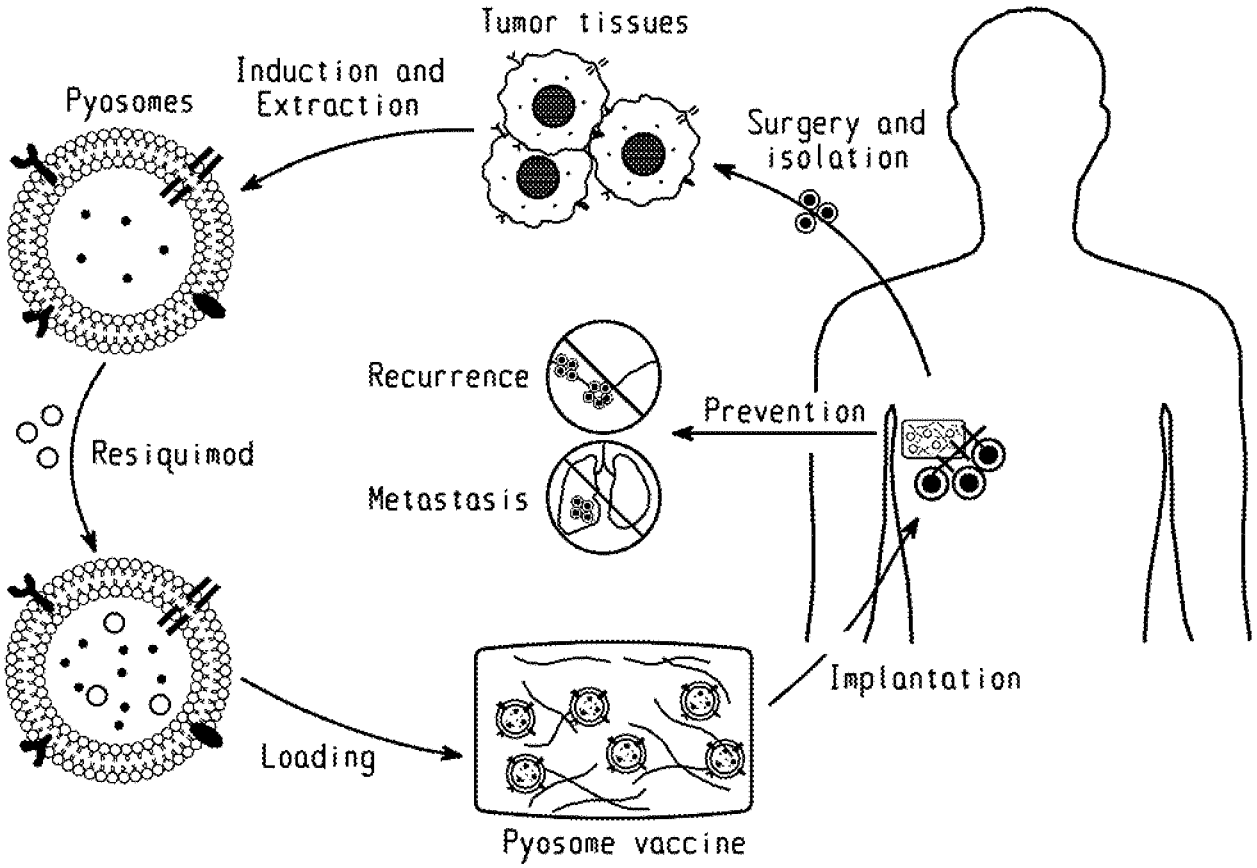
Tumor tissues
Induction and Extraction
Pyosomes
Surgery and isolation
Recurrence
Prevention
Resiquimod
Metastasis
Implantation
Loading
Pyosome vaccine

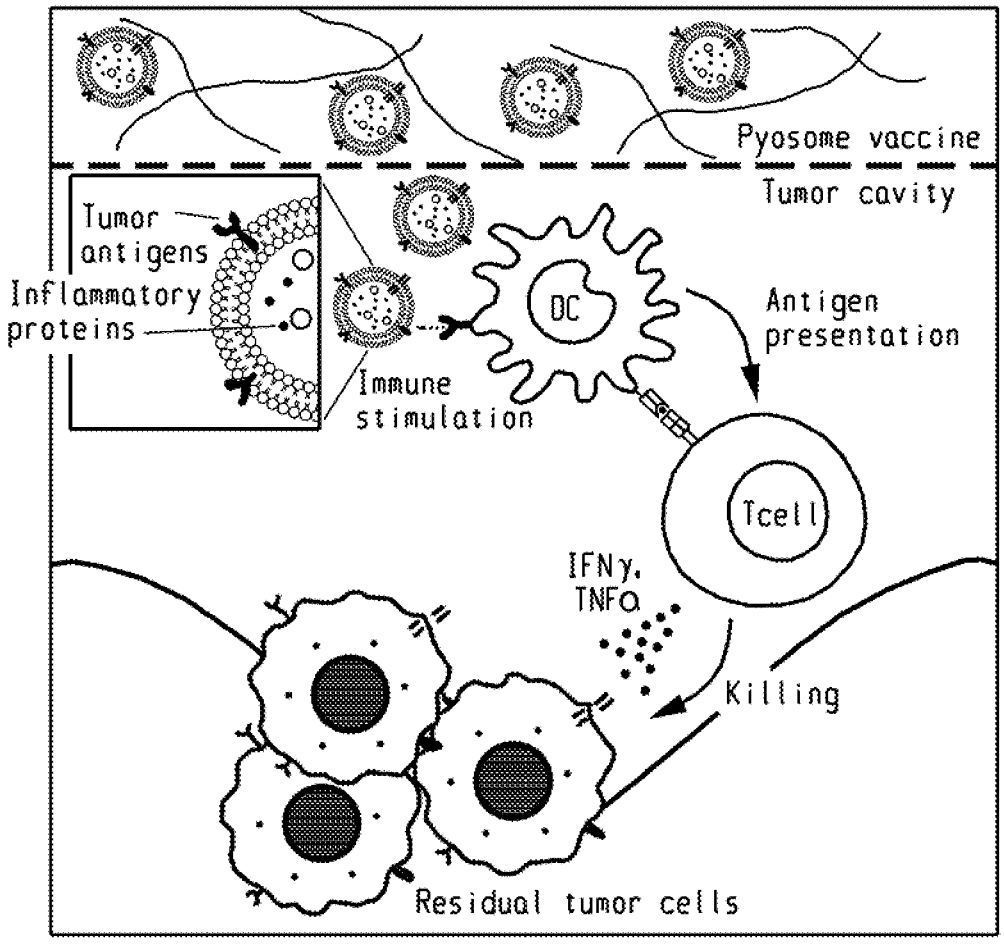
Pyosome vaccine
Tumor cavity
Tumor antigens
Inflammatory proteins
DC
Antigen presentation
Immune stimulation
Tcell
IFNγ, TNFα
Killing
Residual tumor cells

Fig. 8

INTERNATIONAL SEARCH REPORT

International application No.
PCT/US2025/051190

A. CLASSIFICATION OF SUBJECT MATTER

IPC: ***G01N 33/68*** (2025.01); ***G01N 1/40*** (2025.01); *A61K 39/39* (2025.01)

CPC: ***G01N 33/6842; G01N 1/40; A61K 9/1271;*** *A61K 39/39; A61K 2039/555; G01N 2001/4083*

According to International Patent Classification (IPC) or to both national classification and IPC

B. FIELDS SEARCHED

Minimum documentation searched (classification system followed by classification symbols)

See Search History Document

Documentation searched other than minimum documentation to the extent that such documents are included in the fields searched

See Search History Document

Electronic data base consulted during the international search (name of data base and, where practicable, search terms used)

See Search History Document

C. DOCUMENTS CONSIDERED TO BE RELEVANT

Category*	Citation of document, with indication, where appropriate, of the relevant passages	Relevant to claim No.
	CN 118421562 A (SECOND XIANGYA HOSPITAL OF CENTRAL SOUTH UNIVERSITY) 02 August 2024 (02.08.2024)	
X	English translation para [0004]; [0007]; [0011]; [0018]; [0052]; [0053]; [0054]; [0055]	1-9, 14/(1-9)
Y	English translation para [0004]; [0007]; [0011]; [0018]; [0052]; [0053]; [0054]; [0055]	10-13, 14/(10-13)
	US 2023/0241244 A1 (THE REGENTS OF THE UNIVERSITY OF CALIFORNIA) 03 August 2023 (03.08.2023)	
Y	para [0255]; [0607]	10, 14/10
	US 2021/0113678 A1 (ENTEROME S.A.) 22 April 2021 (22.04.2021)	
Y	para [0286]-[0288]; [0323]; [0446]	12-13, 14/(12-13)
	JIANG et al. MiR-21-5p Induces Pyroptosis in Colorectal Cancer via TGFBI. Frontiers in Oncology, 05 February 2021, Vol. 10, Article 610545	
Y	pg 9, col 1, para 1; pg 9, col 1, para 2	11, 14/11

☐ Further documents are listed in the continuation of Box C. ☐ See patent family annex.

* Special categories of cited documents:

"A" document defining the general state of the art which is not considered to be of particular relevance

"D" document cited by the applicant in the international application

"E" earlier application or patent but published on or after the international filing date

"L" document which may throw doubts on priority claim(s) or which is cited to establish the publication date of another citation or other special reason (as specified)

"O" document referring to an oral disclosure, use, exhibition or other means

"P" document published prior to the international filing date but later than the priority date claimed

"T" later document published after the international filing date or priority date and not in conflict with the application but cited to understand the principle or theory underlying the invention

"X" document of particular relevance; the claimed invention cannot be considered novel or cannot be considered to involve an inventive step when the document is taken alone

"Y" document of particular relevance; the claimed invention cannot be considered to involve an inventive step when the document is combined with one or more other such documents, such combination being obvious to a person skilled in the art

"&" document member of the same patent family

Date of the actual completion of the international search	Date of mailing of the international search report
17 December 2025 (17.12.2025)	**13 February 2026 (13.02.2026)**

Name and mailing address of the ISA/US	Authorized officer
COMMISSIONER FOR PATENTS **MAIL STOP PCT, ATTN: ISA/US** **P.O. Box 1450** **Alexandria, VA 22313-1450** **UNITED STATES OF AMERICA**	**HARRY KIM**
Facsimile No. **571-273-8300**	Telephone No. **PCT Help Desk: 571-272-4300**

INTERNATIONAL SEARCH REPORT

International application No.
PCT/US2025/051190

Box No. I Nucleotide and/or amino acid sequence(s) (Continuation of item 1.c of the first sheet)

1. With regard to any nucleotide and/or amino acid sequence disclosed in the international application, the international search was carried out on the basis of a sequence listing:
   a. ☑ forming part of the international application as filed.
   b. ☐ furnished subsequent to the international filing date for the purposes of international search (Rule 13*ter*.1(a)),
      ☐ accompanied by a statement to the effect that the sequence listing does not go beyond the disclosure in the international application as filed.

2. ☐ With regard to any nucleotide and/or amino acid sequence disclosed in the international application, this report has been established to the extent that a meaningful search could be carried out without a WIPO Standard ST.26 compliant sequence listing.

3. Additional comments:

INTERNATIONAL SEARCH REPORT

International application No.
PCT/US2025/051190

Box No. II Observations where certain claims were found unsearchable (Continuation of item 2 of first sheet)

This international search report has not been established in respect of certain claims under Article 17(2)(a) for the following reasons:

1. ☐ Claims Nos.:
because they relate to subject matter not required to be searched by this Authority, namely:

2. ☐ Claims Nos.:
because they relate to parts of the international application that do not comply with the prescribed requirements to such an extent that no meaningful international search can be carried out, specifically:

3. ☑ Claims Nos.: **18-23**
because they are dependent claims and are not drafted in accordance with the second and third sentences of Rule 6.4(a).

Box No. III Observations where unity of invention is lacking (Continuation of item 3 of first sheet)

This International Searching Authority found multiple inventions in this international application, as follows:

This application contains the following inventions or groups of inventions which are not so linked as to form a single general inventive concept under PCT Rule 13.1.

Group I: Claims 1-14, directed to a method of preparing isolated pyosomes (and the pyosome product therefrom), by treating an ex-vivo tumor cell with a pyroptosis-inducing agent under conditions for the tumor cell to undergo pyroptosis and produce pyosomes, and isolating the pyosomes.

Group II: Claims 15-17, directed to a pharmaceutical composition comprising ex-vivo tumor cell derived pyosomes loaded with an immunostimulant and a pharmaceutically acceptable carrier.

1. ☐ As all required additional search fees were timely paid by the applicant, this international search report covers all searchable claims.

2. ☐ As all searchable claims could be searched without effort justifying additional fees, this Authority did not invite payment of additional fees.

3. ☐ As only some of the required additional search fees were timely paid by the applicant, this international search report covers only those claims for which fees were paid, specifically claims Nos.:

4. ☑ No required additional search fees were timely paid by the applicant. Consequently, this international search report is restricted to the invention first mentioned in the claims; it is covered by claims Nos.: **1-14**

Remark on Protest

☐ The additional search fees were accompanied by the applicant's protest and, where applicable, the payment of a protest fee.

☐ The additional search fees were accompanied by the applicant's protest but the applicable protest fee was not paid within the time limit specified in the invitation.

☐ No protest accompanied the payment of additional search fees.